DEUTSCHES ELEKTRONEN-SYNCHROTRON DESY

DESY 79/21
April 1979

受入
79-6-226
高工研図書室

QUANTUM CHROMODYNAMICS AND JETS IN e^+e^-

by

P. Hoyer and P. Osland
NORDITA, Copenhagen

H. G. Sander
I. Physikalisches Institut, TH Aachen

T. F. Walsh
Deutsches Elektronen-Synchrotron DESY, Hamburg

P. M. Zerwas
Institut für Theoretische Physik, TH Aachen
and
Deutsches Elektronen-Synchrotron DESY, Hamburg

NOTKESTRASSE 85 · 2 HAMBURG 52

To be sure that your preprints are promptly included in the
HIGH ENERGY PHYSICS INDEX ,
send them to the following address (if possible by air mail) :

DESY
Bibliothek
Notkestrasse 85
2 Hamburg 52
Germany

Quantum Chromodynamics and Jets in e^+e^-

P. Hoyer
NORDITA, Copenhagen
P. Osland
NORDITA, Copenhagen

H.G. Sander
I. Phys. Institut, TH Aachen

T.F. Walsh
DESY, Hamburg

P.M. Zerwas
Inst. f. Theor. Physik, TH Aachen[+]
and DESY, Hamburg

Abstract

We discuss implications of perturbative QCD for the structure of jets in e^+e^- annihilation above 10 GeV CM energy. (i) A strong asymmetry in the transverse momentum distribution in $e^+e^- \rightarrow$ 2 jets originates from lowest order gluon bremsstrahlung; one jet broadens and the other does not. (ii) Since the gluon is flavor neutral, quantum number correlations between the hadrons in the two jets are smaller than predicted by the parton model. (iii) Jet distributions in QCD are compared with scalar gluon theories. (iv) Three jet structure begins to emerge around 10-15 GeV CM energy. It should be clearly visible in low thrust or high sphericity data at E_{CM} = 30 GeV.

[+] permanent address

I. Introduction

Multiple jets in e^+e^- annihilation (and elsewhere) are a likely feature of any field theory /1/. Thus one expects on quite general grounds that the presently observed bounded $p_\perp$ e^+e^- jets will broaden at high energy. Eventually, a multiple jet structure may emerge within the angular spread of a low energy jet. Perturbative quantum chromodynamics /2/ can predict how this occurs. Up to order $\alpha_s(Q^2)/\pi$ (where $\alpha_s(Q^2) = 12\pi/(33-2N_f)\log Q^2/\Lambda^2$ is the short distance, $L \sim 1/Q$, coupling of the theory for N_F quark flavors and $\Lambda \approx \frac{1}{2}$ GeV) the elementary processes involving QCD quanta are /3/ (Fig. 1.)

$$e^+e^- \rightarrow q\bar{q} \rightarrow \text{hadrons} \qquad (1)$$

$$e^+e^- \rightarrow q\bar{q}G \rightarrow \text{hadrons} \qquad (2)$$

Distributions of global quantities (spheriocity, thrust, angular asymmetries) have been worked out for these elementary processes in /3-7/.

Our aim in this paper is to develop predictions from lowest order perturbative QCD which will allow one to verify some essential features of the theory, viz

(i) The jet broadening due to gluon bremsstrahlung in (2). This takes place in one of the two jets and not in both and results finally in the appearance of a third jet. (Higher order processes such as $e^+e^- \rightarrow qG + \bar{q}G$ /8/ would of course lead to broadening of both jets, but should be unimportant at low energy [+]). We find that lowest order jet broadening is dramatic above

[+] Multijets are important at high energy despite the smallness of α_s. This is because the angular size of a jet from a single gauge quantum decreases as E^{-1}_{quantum} while $\alpha_s \sim (\ln E)^{-1}$.

$Q = 2E_B$ = 30 GeV CM energy, and it increases rapidly with Q^2.

(ii) The flavor neutrality of gluons. We study quantum number correlations in reactions (1) and (2). Since the gluon is flavor neutral it reduces the tendency of fast particles in the two jets to carry opposite charge.

(iii) The vector nature of the gluon in (2). The orientations of the $q\bar{q}G$ plane with respect to the e^+e^- colliding beam axis depends on the spin of the gluon. The resulting asymmetries can in principle be used to check the vector nature of the QCD gauge quanta. For this purpose we confront the vector gluon theory to a scalar gluon theory /3/,/9/.

(iv) The <u>explicit</u> three-jet structure of (2) at high energy and for events with high sphericity and low thrust. The three-jet rate is suppressed by $O(\alpha_s/\pi)$ and by the vanishing phase space when sphericity or thrust reaches its extremum (symmetrical or "star" events).

As to the significance of (i) to (iii) for QCD some reservations are appropriate. The mere existence of jet broadening effects is no direct evidence for QCD but is expected in any field theory. It is essential to check that the jet spreading and, most important, the appearance of 3 jet structures is due to the radiation of flavorless vector quanta. (The experimental verification of the effects mentioned in (i) to (iii) is a necessary condition for perturbative QCD to be valid but not a sufficient one.)

One problem for these studies is the appearance of new flavor thresholds. We have put no weight in this paper on jet broadening due to $e^+e^- \rightarrow b\bar{b} \rightarrow$ hadrons, where $e_b = -1/3$ and $m_b = 5$ GeV. This is because the $b\bar{b}$ threshold above $\Upsilon(9.46)$

gives $\Delta R/R \approx 10$ % at high energies, $R = \sigma_{had}/\sigma_{\mu\bar{\mu}}$. Besides this, $< p_\perp >$ increases above $b\bar{b}$ threshold, but the increase is the same for both jets and is Q^2 independent for large enough Q^2. This is quite unlike the one-sided jet broadening due to gluon bremsstrahlung. On the other hand, a new $t\bar{t}$ threshold, $e_t = 2/3$, would complicate the test of our predictions for $Q^2 \sim 4m_t^2$. $\Delta R/R \approx 40$ % and the $p_\perp$ increase is large, due to the large t mass, $m_t \gg m_b$. One either has to go to $Q^2 \gg 4m_t^2$ to test QCD effects or exploit the planarity of the three-quantum state in (2); $e^+e^- \to t\bar{t} \to$ hadrons will not lead to planar events [+].

We present the material as follows. First we derive results which have a minimal dependence on how quarks and gluons fragment (nonperturbatively) into observed hadrons. In the next step we assume the validity of Feynman's fragmentation picture of quark and gluon jets. In this Section we concentrate on jet broadening, with a remark on the change of charge correlations due to gluon bremsstrahlung. It turns out that at high energies ($Q \gtrsim 30$ GeV) jet broadening has no serious model dependence. Our results test perturbative quantum chromodynamics and not our assumptions. Finally, we present the results of a Monte Carlo model which includes both $q\bar{q}$ and $q\bar{q}G$ states, the quanta fragmenting in a sequential way to hadrons /11,12/. We compare the results from this model with our earlier analytic calculations. The agreement is satisfying. In addition, this model has other applications.

II. Minimal Dependence on Nonperturbative Effects

As discussed in Refs. /4,13/, quantities linear in momenta are least model

[+] For a study of $b\bar{b}$ and $t\bar{t} \to$ hadrons see Ref. /10/ and the Monte Carlo programs developed by these authors. (Such a program has also been prepared by T. Meyer.)

dependent. These are independent of how quarks and gluons fragment because a linear sum of hadron momenta in a jet is just the gauge quantum momentum (as $Q \to \infty$).

An appropriate measure of jet broadening is thus given as follows. The reference axis is taken to be the thrust axis $T = \max(x_1, x_2, x_3)$ where $x_i = E_i / E_B$ (E_i and E_B are the q or G energy and the e^+e^- beam energy). Then we define a variable $x_\perp = x_i \sin\theta_i$, the <u>jet momentum perpendicular to the T axis</u> (Fig. 2.) In terms of hadron momenta $p_\perp^i$ ($\perp$ to the T axis), /13/

$$x_\perp = \frac{1}{2} \sum_i |\vec{p}_\perp^{\,i}| / E_B \tag{3}$$

summed over all hadrons i. (Of course, there is a finite $p_\perp$ $q\bar{q} \to 2$ jet non-perturbative contribution $x_\perp \sim \langle p_\perp \rangle N_{had} / E_B \to 0$.)

Up to $O(\alpha_s)$

$$\frac{1}{\sigma} \frac{d\sigma}{dx_\perp} = \frac{1}{\sigma_0} \int_{T_{min}}^{T_{max}} dT \; \frac{d\sigma(q\bar{q}G)}{dx_\perp dT} \tag{4}$$

where the integral is obtained from

$$\frac{1}{\sigma_0} \frac{d\sigma(q\bar{q}G)}{dx_q \, dx_{\bar{q}}} = \frac{2}{3} \frac{\alpha_s(Q^2)}{\pi} \frac{x_q^2 + x_{\bar{q}}^2}{(1-x_q)(1-x_{\bar{q}})} \tag{5}$$

the cross section for $e^+e^- \to q\bar{q}G$ normalized to $e^+e^- \to q\bar{q}$ /3/, and $x_\perp^2 = 4(1-x_q)(1-x_{\bar{q}})(1-x_G)/T^2$. The limits of integration are $T_{max} = 1 - x_\perp^2$ and T_{min}, the solution of

$$x_\perp^2 = \frac{4}{T_{min}^2} (1 - T_{min})^2 (2T_{min} - 1) \tag{6}$$

where $2/3 \leq T_{min} \leq T_{max} \leq 1$. The $x_\perp$ distribution is shown in Fig. 3.

Although $d\sigma/dx_\perp$ diverges as $x_\perp \to 0$, moments $\langle x_\perp^n \rangle$ of $x_\perp$ are finite and are predictible in perturbative QCD. Despite the fact that the moments are finite, their numerical value can depend on low $x_\perp$ where nonperturbative effects are important. Thus in fig. (4) we exhibit moments with a cut on $x_\perp$, $x_\perp \geq x_\perp^{min}$,

$$\langle x_\perp^n \rangle = \frac{1}{\sigma_0} \int_{x_\perp^{min}}^{1/\sqrt{3}} dx_\perp \int_{T_{min}}^{1-x_\perp^2} dT \; x_\perp^n \; \frac{d\sigma(q\bar{q}G)}{dT\, dx_\perp} \tag{7}$$

Observation of a scaling $\frac{1}{\sigma}\frac{d\sigma}{dx_\perp} \ln Q^2$ and energy independence of $\langle x_\perp^n \rangle \ln Q^2$ would be evidence for the transverse momentum jet broadening of QCD.

A model independent test that gluons have no flavor can be constructed for the high energy regime. We consider the following <u>weighted charge correlation.</u> First we suppose that even if three jets from $e^+e^- \to q\bar{q}G$ are not all identifiable, at least two are. Except near $T = 2/3$ events consist of a hard jet (along the T axis) and a less hard one at an angle to the T axis (see Fig. 2.). The third jet is expected to deliver many low energy particles; it will be hard to reconstruct. Having identified the two hard jets we order them by E(jet 1) > E(jet 2). (These jet axes may be identifiable by cutting out low momentum particles not associated with any jet, by limiting the event multiplicity, or in some other way). Now we construct the average charge correlation

$$C(T) = \langle Q_1 Q_2 \rangle = \left\langle \left[\sum_{i \in 1} e_i \frac{z_i}{x_1} \right] \left[\sum_{j \in 2} e_j \frac{z_j}{x_2} \right] \right\rangle \tag{8}$$

as a function of thrust T. (Any power $(z/x_j)^p$ is also acceptable /11/,

though $p > 0$ is desirable). In (8) $z_{i,j}$ is the scaled momentum of particle i,j in jet 1,2 and $e_{i,j}$ its charge. At high energy, $\langle Q_1 Q_2 \rangle$ is a scaling quantity (ignoring log scaling violations) and is independent of the jet momentum. Because of this scaling property and the absence of gluon flavor,

$$\langle Q_q Q_{\bar{q}} \rangle = C(1)$$
$$\langle Q_q Q_G \rangle = \langle Q_{\bar{q}} Q_G \rangle = 0 \tag{9}$$

(At T = 1 we have $e^+e^- \to q\bar{q}$ only). Hence $C(T)$ is given by $C(1)$ times the probability that jets 1 and 2 are q and $\bar{q}$,

$$\frac{C(T)}{C(1)} = \frac{2\int_{(2-T)/2}^{T} dx\ \rho_0(T,x)}{\int_{2(1-T)}^{T} dx \left\{ \rho_0(T,x) + \rho_0(x, 2-T-x) + \rho_0(2-T-x, T) \right\}} \tag{10}$$

where we used the abbreviation

$$\rho_0(x_q, x_{\bar{q}}) = \frac{x_q^2 + x_{\bar{q}}^2}{(1-x_q)(1-x_{\bar{q}})} \tag{11}$$

The ratio $C(T)/C(1)$ is shown in Fig. 5. $C(1)$ is experimentally accessible in two-jet events with maximum thrust $T \to 1$. In the Feynman-Field parton-jet model it is given (as an incoherent 4 : 1 : 1 mixture of u, d, s quarks) by [+)]

$$C(1) = -.012 \pm .003 \ (p=1)\ ;\ C(1) = -.062 \pm .006 \ (p=.5)\ ;\ C(1) = -.29 \pm .02 \ (p=.2) \tag{12}$$

At fixed T and high energy three jets will be visible. Then one can study other correlations, e.g. the correlation between the most and the least

---

[+)] For completeness, we show $C(1)$ for various p, not just p = 1. We took E_{CM} = 90 GeV.

energetic jet, $\langle Q_1 Q_3 \rangle$. This is expected to be very much smaller than $\langle Q_1 Q_2 \rangle$ because the least energetic jet is almost always a flavorless G jet (as long as T is not near 2/3).

In order to test the spin of the bremsstrahlung gluon we study the angular dependence of the three-jet cross section. The orientation of the hadron plane spanned by the 3 momentum vectors of q, $\bar{q}$, G, is conveniently described by θ , the angle between the incoming electron and one of the emitted quanta, and χ , the angle between the hadron plane and the plane spanned by the e^+e^- beam axis and the momentum of the quantum defining θ . Expressed in terms of helicity cross-sections (U = unpolarized transverse, L = longitudinally polarized; T, I = +1/-1, 0/1 interference terms) the most general form for $e^+e^- \to q\bar{q}G$ is /7/

$$2\pi \frac{d\sigma}{dx_q dx_{\bar{q}} d\cos\theta d\chi} = \frac{3}{8}(1+\cos^2\theta)\frac{d\sigma^U}{dx_q dx_{\bar{q}}} + \frac{3}{4}\sin^2\theta \frac{d\sigma^L}{dx_q dx_{\bar{q}}}$$

$$+ \frac{3}{4}\sin^2\theta\cos 2\chi \frac{d\sigma^T}{dx_q dx_{\bar{q}}} - \frac{3}{2\sqrt{2}}\sin 2\theta\cos\chi \frac{d\sigma^I}{dx_q dx_{\bar{q}}} \qquad (13)$$

The results of $d\sigma^i$ for vector gluons are listed in Ref. /7/ and we will confront them with the scalar gluon case. Choosing the gluon momentum as the reference axis (defining θ), for scalar gluons only the unpolarized transverse cross section is nonzero

$$\frac{d\sigma^U}{dx_q dx_{\bar{q}}} = \frac{g^2}{4\pi}\frac{\sigma_0}{4\pi}\frac{x_G^2}{(1-x_q)(1-x_{\bar{q}})} \qquad (14)$$

with σ_0 being the $e^+e^- \to q\bar{q}$ cross section (three colors); g is the Yukawa

coupling constant. $d\sigma^U/dx_q dx_{\bar{q}}$ coincides with the general angle integrated cross section $d\sigma/dx_q\, dx_{\bar{q}}$. Unlike the vector gluon case we don't have an azimuthal angular dependence on χ (with G as axis) for scalar gluons, and the θ dependence is purely $(1 + \cos^2\theta)$. Since it is exceedingly difficult to determine the gluon axis (e.g. via quantum numbers), we also list the cross sections if the quark or antiquark momentum is chosen as reference axis. They are required in calculating thrust distributions.

$$\frac{d\sigma^U}{dx_q dx_{\bar{q}}} = A\left(x_G^2 - \tfrac{1}{2}x_\perp^2\right) \qquad \frac{d\sigma^I}{dx_q dx_{\bar{q}}} = A\,\frac{1}{2\sqrt{2}}\,x_\perp x_G^{\parallel}$$

$$\frac{d\sigma^L}{dx_q dx_{\bar{q}}} = A\,\tfrac{1}{2}x_\perp^2 \qquad \frac{d\sigma^T}{dx_q dx_{\bar{q}}} = \frac{1}{2}\,\frac{d\sigma^L}{dx_q dx_{\bar{q}}} \tag{15}$$

$$A = \frac{g^2}{4\pi}\,\frac{\sigma_0}{4\pi}\,\frac{1}{(1-x_q)(1-x_{\bar{q}})}$$

$x_\perp$ denotes the absolute value of the transverse momentum of the antiquark relative to the quark axis (and vice versa); $-x_G^{\parallel}$ is the longitudinal momentum of the gluon relative to the quark (antiquark) axis. This complicated θ and χ dependence of the cross section is of course spurious and related to the unfavorable choice of quark or antiquark momentum as reference axis. Provided the gluon jet could be identified we find a very clean way of testing the spin of the gluons. For scalar gluons we predict isotropic hadron distributions around the gluon jet axis. For vector gluons we expect nonzero azimuthal asymmetries for the average quantities $\langle\cos\chi\rangle$/7/ and $\langle\cos 2\chi\rangle$/6/,/7/. However, if we are forced to choose thrust as the reference axis this vector-scalar difference gets largely washed out. In Fig. 6 we present $d\sigma^i/dT$ (for i = U, L, T, I), comparing scalar with vector gluons, the Yukawa coupling constant adjusted so that $d\sigma^U/dT$(scalar) = $d\sigma^U/dT$ (vector) at T = .8.

χ is now the azimuthal angle of the second most energetic jet about the thrust axis. $d\sigma^{L,T}/dT$ is larger in the scalar gluon case than in the vector gluon case, $d\sigma^{I}/dT$ is smaller.

III. Including Quark and Gluon Fragmentation

In the preceding section we tried as much as possible to avoid dependence on details which may obscure QCD tests: how quarks and gluons fragment into hadrons and how the two-jet and three-jet final states merge into one another. However, there are many quantities of experimental relevance which do depend on just these matters. The mean $\langle p_\perp^2 \rangle$ in a broadening jet is one example. Moreover a central issue - at what energy QCD jet broadening is clear and unmistakable - depends in an essential way on the nonperturbative hadronization mechanism.

We begin by discussing the global $\langle p_\perp^2 \rangle$ in e^+e^- events, which we try to deal with in a reasonably model independent way. Next we treat <u>in extenso</u> the mean $\langle p_\perp^2(z) \rangle$ relative to the thrust axis of a single hadron with scaled momentum $z = p_{had}/E_B$. This turns out to be insensitive to quark and gluon fragmentation and fundamental theoretical uncertainties only for $Q \gtrsim 30$ GeV. Below this energy there appears a significant problem arising from the precise way two- and three-jet mechanisms merge at high thrust (nearly collinear or soft gluons in (2)). However, we show how one can avoid this problem by studying events of low thrust only. $\langle p_\perp^2 \rangle$ in these events depends only on experimentally accessible fragmentation functions and thus provides us with a clean test of perturbative QCD. Finally we return to charge correlations as affected by flavorless gluon bremsstrahlung. The test we propose does not depend on

identifying a second jet as in section II.

One can derive a result on the average transverse momentum which is at least insensitive to the fragmentation mechanism by taking advantage of the cancellation between singularities in diagrams with real and virtual gluons. The collinear and soft gluon divergences which appear in the $O(\alpha_s)$ cross-section for $e^+e^- \to q\bar{q}G$ are cancelled in σ_{tot} by corresponding singularities in the $e^+e^- \to q\bar{q}$ cross-section /14/. Such cancellations always occur between energy-degenerate states /15/. Now it is plausible to assume that the hadrons produced from states consisting of a single quark and of a quark plus a collinear or soft gluon, will have the same average transverse momentum, provided we assume that the nonperturbative transverse momentum of quark and gluon fragments are the same. A soft gluon, on the other hand, cannot produce any hadrons. The cancellation of singularities between real and virtual processes will then work in the same way for the average transverse momentum as for σ_{tot}, and we get a cut-off independent result +).

The $p_\perp^2$ of a hadron which is a fragment of a parton j ($j = q, \bar{q}$ or G), whose momentum p_j makes an angle θ_j with the thrust axis is, averaging over the nonperturbative (NP) fragmentation

$$\langle p_\perp^2 \rangle_j - \langle p_\perp^2 \rangle_{NP} = \left[\langle z^2 \rangle_{NP} p_j^2 - \frac{1}{2} \langle p_\perp^2 \rangle_{NP} \right] \sin^2\theta_j \qquad (16)$$

Here, z measures the scaled longitudinal hadron momentum parallel to the jet axis; $\langle z^2 \rangle_{NP}$ and $\langle p_\perp^2 \rangle_{NP}$ characterize the NP fragmentation process,

+) The cancellations only work in $p_\perp$-averages that are integrated over all z as the weight factors for the collinear states will otherwise depend on the relative momenta.

and are assumed to be the same for quarks and gluons. The overall average hadron transverse momentum is obtained by summing over parton species j and integrating over all $q\bar{q}G$ configurations. In order to (approximately) account for the number of hadrons produced by a given parton we give a relative weight to the $q,\bar{q}$ and G contributions which is proportional to the parton energies. The average transverse momentum of hadrons obtained in this way from Eq. (16) is

$$\langle p_\perp^2\rangle - \langle p_\perp^2\rangle_{NP} = \frac{1}{3}\frac{\alpha_s}{\pi}\int_{2/3}^{1} dT \int_{2(1-T)}^{T} dx \left[2\frac{T^2+x^2}{(1-T)(1-x)} + \frac{x^2+(2-T-x)^2}{(1-x)(T+x-1)}\right]\cdot\left[\frac{Q^2}{4}\langle \xi^2\rangle_{NP} - \frac{1}{2}\frac{\langle p_\perp^2\rangle_{NP}}{x(2-T-x)}\right] x_\perp^2 (2-T) \qquad (17)$$

where $x_\perp^2 = 4(1-T)(1-x)(T+x-1)/T^2$. Numerically, from (17),

$$\langle p_\perp^2\rangle = \langle p_\perp^2\rangle_{NP} + \frac{\alpha_s(Q^2)}{3\pi}\left[.281\,\langle \xi^2\rangle_{NP} Q^2 - 2.55\,\langle p_\perp^2\rangle_{NP}\right] \qquad (18)$$

It follows from (18) that the energy scale at which the QCD jet broadening sets in, $p_\perp^2 \sim \alpha_s Q^2$, is determined by the ratio $\langle p_\perp^2\rangle_{NP}/\langle \xi^2\rangle_{NP}$. In Fig. 7. we have used $\langle p_\perp^2\rangle_{NP} = .177\,GEV^2$ and $\langle \xi^2\rangle_{NP} = .0416$ /16/. The broadening sets in around Q = 10 to 15 GeV and grows rapidly, becoming a 100 % effect at Q = 30 GeV. Numerically, for 3 flavors

$$\frac{\langle p_\perp^2\rangle}{\langle p_\perp^2\rangle_{NP}} = 1 + \frac{1}{\ln Q/\Lambda}\left[\left(\frac{Q}{14.3}\right)^2 - .189\right]$$

A completely analogous analysis can be done for $\langle p_\perp^4\rangle$. We obtain

$$\langle P_\perp^4 \rangle = \langle P_\perp^4 \rangle_{NP} + \frac{\alpha_s(Q^2)}{3\pi} \left[.00735 \langle \xi^4 \rangle_{NP} Q^4 + \right. \tag{19}$$

$$\left. + .848 \langle \xi^2 p_\perp^2 \rangle_{NP} Q^2 - 4.12 \langle P_\perp^4 \rangle_{NP} \right]$$

Using $\langle \xi^4 \rangle_{NP} = .0086$, $\langle \xi^2 P_\perp^2 \rangle_{NP} = .0074\,GEV^2$, $\langle P_\perp^4 \rangle_{NP} = .077\,GEV^4$ we find (Fig. 7) that the broadening begins around $Q \approx 10$ GeV and grows extremely rapidly. It is clear, however, that high statistics is required to measure $\langle P_\perp^4 \rangle$ experimentally.

Rewriting Eq. (16) as

$$\langle P_\perp^2 \rangle = \frac{1}{4} Q^2 z^2 \sin^2\theta_j + \langle P_\perp^2 \rangle_{NP} \left[1 - \frac{3}{2} \sin^2\theta_j \right] \tag{20}$$

we can exploit this equation further in order to calculate the <u>average transverse momentum</u> $\langle P_\perp^2(z) \rangle$ of a single hadron relative to the T axis <u>as a function of its scaled momentum</u> $z = p/E_B$. By inspecting Figs. 1 and 2 it is obvious that in lowest order QCD one jet broadens and not both. We assume from now on that events are ordered. We suppose that one hemisphere (the dividing plane being perpendicular to the thrust axis) contains the "narrower" jet, the second hemisphere the " broader"jet. (This ordering should be carried out using only hadrons with $z \gtrsim$ some z_0, the low energy hadrons being cut out.) One defines a truncated thrust

$$T' = \max \left\{ \sum_{\substack{i \in H \\ z \geq z_0}} |p_\parallel^i| \Big/ \sum_{\substack{i \in H \\ z \geq z_0}} |\vec{p}^{\,i}| \right\}$$

where H refers to the hemisphere around a directed axis relative to which $p_\parallel^i$ is defined.) [+)]

[+)] A jet finding algorithm which does not correctly identify the axis of the narrow jet can lead to a spurious "broadening" of both jets.

Perturbative QCD predicts that the narrow jet defined by T' shows no increase up to and <u>including</u> $O(\alpha_s)$. The jet in the hemisphere opposite T' broadens, $\langle p_\perp^2 \rangle \sim O(\alpha_s Q^2)$. The single hadron $\langle p_\perp^2(z) \rangle$ is obtained by weighting Eq. (20) by the probability to find a jet at an angle θ_j relative to the T axis and containing a hadron of fractional momentum z (or z/x_j relative to the jet),

$$\langle p_\perp^2(z) \rangle = \Big[\frac{1}{4} z^2 Q^2 \sum_j \int d\sigma_j \frac{1}{x_j} D_j^h\Big(\frac{z}{x_j}\Big) \sin^2\theta_j +$$

$$+ \sum_j \int d\sigma_j \frac{1}{x_j} D_j^h\Big(\frac{z}{x_j}\Big) \langle p_\perp^2\Big(\frac{z}{x_j}\Big)\rangle_{NP} \Big(1 - \frac{3}{2}\sin^2\theta_j\Big)\Big] \times \quad (21)$$

$$\times \Big[\sum_j \int d\sigma_j \, D_j^h(z) \Big]^{-1}$$

where j runs over q and $\bar{q}$ at $\theta_j = 0$ (i.e. thrust T = 1) and $q\bar{q}G$ at non-zero θ_j (i.e. thrust $T < 1$). The latter probability is $O(\alpha_s)$ relative to the former. We simplify (21) by dropping terms of order $\alpha_s \langle p_\perp^2 \rangle_{NP}$ relative to $\langle p_\perp^2 \rangle_{NP}$ and $\alpha_s Q^2$, consistent with having normalized (21) to the nonperturbative $q\bar{q}$ jet cross section.+) In doing this we have to define $e^+e^- \to q\bar{q}G$ (of order α_s) relative to $q\bar{q}$ (of order 1) by a thrust cut: $2/3 \leq T_{q\bar{q}G} \leq T_o$ in the former process and $T = 1$ in the latter. This is necessary for physics reasons. As $T \to 1$, $q\bar{q}G$ merges continuously into a nonperturbative $q\bar{q}$ jet. $q\bar{q}G$ cannot be isolated above some T_o, and we should not refer to this process for $T > T_o$. In perturbation theory, the singular behavior of $q\bar{q}G$ at $T \to 1$ is cancelled by a multiplicative divergent factor in $e^+e^- \to q\bar{q}$ exactly at T = 1. Unfortunately this is of no use to us, as this thrust value is far inside a nonperturbative jet. (Actually, the <u>hadronic</u> $d\sigma/dT$ even vanishes at T = 1, owing to phase space.) Of course, (21) is finite for $T_o = 1$, so we are justified

+) Up to this order it is also consistent to ignore scaling violations in D_j^h, as we will do.

in ignoring all this at high energies where $1 - T_o \sim 1/Q^2 \to 0$. However, we will see that this merging of $q\bar{q}G$ into a $q\bar{q}$ jet is an important effect at low energies. Keeping this in mind, we find [+)]

$$\langle P_\perp^2(z)\rangle - \langle P_\perp^2(z)\rangle_{NP} = \frac{\alpha_s(Q^2)}{\pi} G(z)\, Q^2 \tag{22}$$

with the profile G(z) given by [++)]

$$G(z) = \frac{4z^2}{3}\int_{2/3}^{T_o}\frac{dT}{T^2}\int_{x_L}^{T}\frac{dx}{x^3}\left\{\left[\rho_2(T,x)+\rho_2(x,2-T-x)\right]D_q\left(\frac{z}{x}\right)\right.$$
$$\left. + \rho_2(2-T-x,T)\, D_G\left(\frac{z}{x}\right)\right\} \Big/ D_q(z) \tag{23}$$

where $x_L = \mathrm{MAX}(z, 2(1-T))$ and $\rho_2(x_q, x_{\bar{q}})$ is a generalization of Eq. (11),

$$\rho_n(x_q, x_{\bar{q}}) = \frac{x_q^2 + x_{\bar{q}}^2}{(1-x_q)(1-x_{\bar{q}})}\left[(1-x_q)(1-x_{\bar{q}})(x_q + x_{\bar{q}} - 1)\right]^{n/2} \tag{24}$$

note that the integral vanishes when $z > T_o$, and G(z) is finite for $T_o = 1$.

In the following we set $D_q(z) = (r+1)(1-z)^r/z$ and $D_G = (s+1)(1-z)^s/z$ and take the thrust cut T_o dividing the nonperturbative $e^+e^- \to q\bar{q} \to$ 2 jets from $e^+e^- \to q\bar{q}G$ to be

$$T_o = 0.8 \quad \text{and} \quad T_o = 0.95 \quad (Q = 30\,\mathrm{GeV}) \tag{25}$$

+) A similar quantity has been considered by Schierholz and Kramer using another method /17/.

++) The fragmentation functions for quarks and gluons are averaged over the quark and hadron species: $D_q = \sum_{h,q} D_q^h$, $D_G = \sum_h D_G^h$.

where T_o can be obtained from theoretical estimates . The dependence of our results on T_o measures the degree of theoretical uncertainty. (We will return to this in Sec. IV.) For $T_o = 1$, $\langle p_\perp^2(z)\rangle$ is almost independent of the form of $D_q(z)$ and $D_G(z)$. This is shown in Fig. 8a where G(z) is given for various parametrizations of D_G and D_q /18/,/19/. The dependence on the parametrization, being on the $\pm$ 20 % level, is not serious. (Changing r and s independently does not alter this conclusion.) For completeness' sake we also present on Fig. 8b a comparison of vector and scalar gluon cases /3/.

Fig. 9 shows G(z) for $T_o = 0.8$; $T_o = 0.95$ ($Q = 30$ GeV) and $T_o = 1$ ($Q = \infty$) for $r = s = 2$. From the comparison we conclude that the results are reliable for $Q \geq 30$ GeV and uncertain to perhaps a factor 2 around 15 GeV because of the strong dependence on T_o. Finally, Fig. 10 presents our results for $\langle p_\perp^2(z)\rangle$ including the asymmetry between the narrow and the broadened jets ($\langle p_\perp^2(z)\rangle_{NP}$ is adopted from section IV). The asymmetry effect is small at $T_o = 0.8$ (nicely agreeing with $\langle p_\perp^2\rangle$ on Fig. 7). On the other hand, the predicted broadening sets in quite dramatically and is unmistakeable at $Q \geq 30$ GeV.

The major uncertainty in the above analysis lies in the appearance of a thrust cut-off parameter T_o. In order to have a clean test of perturbative QCD it would be highly desirable to eliminate this fundamental uncertainty. Indeed we can escape this cut-off dependence by considering only events in the perturbative regime $2/3 \leq T \leq T_{max} < T_o$ (with T_{max} independent of Q.) These are entirely $q\bar{q}G$ events normalized to the known $e^+e^- \rightarrow q\bar{q}G$ cross section in the

region $2/3 \leq T \leq T_{max}$. To eliminate the uncertainty in T_o we just choose T_{max} small enough.

We can now define moments of the transverse momentum, for events with $2/3 \leq T \leq T_{max}$,

$$\langle p_\perp^n(z)\rangle = Q^n z^n \int_{2/3}^{T_{max}} dT \int_{x_L}^{T} \frac{dx}{x(xT)^n} \left\{ \left[\rho_n(T,x) + \rho_n(x, 2-T-x)\right] D_q\left(\frac{z}{x}\right) \right.$$

$$\left. + \rho_n(2-T-x,T)\, D_G\left(\frac{z}{x}\right) \right\} \Big/ \int_{2/3}^{T_{max}} dT \int_{x_L}^{T} \frac{dx}{x} \left\{ n \to 0 \right\} \tag{26}$$

with $x_L = MAX(z, 2(1-T))$. The z-integrated form is

$$\langle p_\perp^n \rangle_{T_{max}} = Q^n \int_{2/3}^{T_{max}} \frac{dT}{T^n} \int_{2(1-T)}^{T} dx \left\{ \left[\rho_n(T,x) + \rho_n(x, 2-T-x)\right] \langle z^n \rangle_q \right.$$

$$\left. + \rho_n(2-T-x, T) \langle z^n \rangle_G \right\} \Big/ \int_{2/3}^{T_{max}} dT \int_{2(1-T)}^{T} \frac{dx}{x} \left\{ n \to 0 \right\} \tag{27}$$

where

$$\langle z^n \rangle_{q,G} = \int_0^1 dz\, z^n\, D_{q,G}(z)$$

(For our numerical results in Figs. 11 and 12 we take $D_q(z) = D_G(z) = z^{-1}(1-z)^2$ for charged pion final states.) A particularly nice quantity to discuss is the first moment ($n = 1$) in Eq. (27) if we sum over all hadrons in the jets, resulting in $\langle z \rangle_{q,G} = 1$ [+)] by momentum conservation and leaving us with the

---

+) This is even independent of logQ violations of Feynman scaling.

hadron multiplicity of the jets as the only parameter. (This is, of course, experimentally accessible.) The result for equal hadron multiplicity in quark and gluon jets is presented in Fig. 12. Clearly, these quantities escape the theoretical uncertainty mentioned above and the scaling laws for the moments of the transverse momentum $\langle p_\perp^n \rangle_{T_{max}} \sim Q^n$ as well as their absolute magnitude provide a theoretically clean test of perturbative QCD.

We now turn to some tests that jet broadening is due to the emission of flavorless gluons. We take a π^+ in the narrow jet (T′ hemisphere) with scaled momentum $0.8 \leq z/T \leq 1$ and calculate the π^+/π^- ratio in the opposite hemisphere. The two-particle distribution for a π^+ in this z/T range is given as

$$\frac{d\sigma(\pi^+\pi)}{dT\,dz} \propto \int \frac{dx}{x} \rho_0(T,x) \sum_q e_q^2 \left[N_q^{\pi^+} D_{\bar{q}}^{\pi}\left(\frac{z}{x}\right) + N_{\bar{q}}^{\pi^+} D_q^{\pi}\left(\frac{z}{x}\right)\right]$$

$$+ \int \frac{dx}{x} \rho_0(x, 2-T-x) \sum_q e_q^2 N_G^{\pi^+} \left[D_q^{\pi}\left(\frac{z}{x}\right) + D_{\bar{q}}^{\pi}\left(\frac{z}{x}\right)\right] \qquad (28)$$

$$+ \int \frac{dx}{x} \rho_0(2-T-x, T) \sum_q e_q^2 \left[N_q^{\pi^+} + N_{\bar{q}}^{\pi^+}\right] D_G^{\pi}\left(\frac{z}{x}\right)$$

We have chosen a π^+ in the T′ hemisphere with $z/T \geq 0.8$ to select out (with large probability) a q = u or $\bar{d}$ parent quark. Then $N_q^{\pi^+} = \int_{.8}^{1} d\xi\, D_q^{\pi^+}(\xi)$ for q = u or $\bar{d}$. (Small amounts of other flavor contributions can easily be taken account of.)

Choosing again $D_q^{\pi^+ + \pi^-}(z) = D_G^{\pi^+ + \pi^-}(z) = z^{-1}(1-z)^2$ and $D_u^{\pi^-} / D_u^{\pi^+} = (1-z)/(1+z)$, we plot in fig. 13 the π^+/π^- ratio /21/

$$C\left(\frac{\pi^+}{\pi^-}; T, z\right) = \frac{d\sigma(\pi^+\pi^+)}{dT\,dz} \Big/ \frac{d\sigma(\pi^+\pi^-)}{dT\,dz} \qquad (29)$$

for $e^+e^- \to q\bar{q}G$ at various T and also for $e^+e^- \to q\bar{q}$. The influence of flavorless gluon bremsstrahlung remains modest in $\zeta'(\pi^+/\pi^-)$. This can be traced back to the fact that bremsstrahlung gluons tend to be soft, enlarging the hadron population in the small z region. It is flavor neutral anyway.

IV. Monte Carlo Model

Now we want to study in a realistic way the interplay of nonperturbative and perturbative jet broadening. We do this using a Monte Carlo model which simulates the jets from quarks and gluons.[+)] The basic ingredients are the following.

(i) We restrict ourselves to u, d and s quarks. (c and b can be included, given a model for their fragmentation and decay /10/.) The jet generator recipe is that of Feynman and Field /11/. We require a minimum jet energy of 2 GeV.

(ii) Gluon jets are treated as a combination of quark antiquark pairs with weight $u\bar{u}:d\bar{d}:s\bar{s} = 2:2:1$ and choosing $3(1-z)^2$ for the primordial decay function.

(iii) The cross section for $e^+e^- \to q\bar{q}G$ is given by QCD (equ. (5)) for $2/3 \leq T \leq T_o$. For $T > T_o$ we set $d\sigma(q\bar{q}G) = 0$. This is the cutoff used to distinguish $e^+e^- \to q\bar{q}G$ from $e^+e^- \to q\bar{q}$.

We now generate $e^+e^- \to q\bar{q} + q\bar{q}G \to$ hadrons. The total $q\bar{q}G$ rate is, from (iii),

$$\sigma(q\bar{q}G) = \int_{2/3}^{T_o} dT \; \frac{d\sigma(q\bar{q}G)}{dT} \tag{30}$$

[+)] This is also being done by D. Drijard (private communication)

By contrast, $(q\bar{q})$ nonperturbative two jets are generated with overall rate

$$\sigma_0 - \left[\sigma(q\bar{q}G) - \frac{\alpha_s(Q^2)}{\pi}\sigma_0\right] = \sigma(q\bar{q}) \tag{31}$$

This is required by conservation of probability. A large probability for hard gluon bremsstrahlung decreases the probability for a $e^+e^- \rightarrow q\bar{q}$ two jet event. (This is the underlying reason for the cancellation of infrared singularities in $q\bar{q}G$ and $q\bar{q}$ which we mentioned earlier.)

We have considered a number of cutoff procedures. The one which we employ here is chosen to give a smooth transition from $q\bar{q}$ to $q\bar{q}G$ in the observed (hadronic) thrust distribution. Let T_o be that thrust value where the pure nonperturbative $q\bar{q}$ distribution is a maximum,

$$\frac{d}{dT}\left[\frac{d\sigma(q\bar{q})_{NP}}{dT}\right]_{T_o} = 0 \tag{31}$$

The perturbative $q\bar{q}G$ process runs from $T = 2/3$ to T_o, and after smearing with quark and gluon jet fragmentation should produce a reasonable $d\sigma/dT$ distribution.

We also considered a minimum scaled transverse momentum of all jets relative to one another, $X_\perp \geq .07$, and a minimum jet energy, $E_j \geq 2$ GeV. This procedure is not successful. It generates too much large $P_\perp$ at low energies. Moreover, the integrated $q\bar{q}G$ cross section is unreasonable (~ 80 % of σ_0 already at $Q = 30$ GeV).

In fig. (14) we show the pure two jet $(1/\sigma)\, d\sigma/dT$.

In fig. (15) we show the corresponding $(1/\sigma)\, d\sigma/dT$ for $e^+e^- \to q\bar{q} + q\bar{q}G$, using the model we have been describing. The cutoff we use leads to $T_o = 0.92, 0.95, 0.98$ at Q = 15, 30, 90 GeV. Correspondingly, $\sigma(q\bar{q}G)/\sigma_0 = 0.17, 0.29, 0.49$.

The asymmetry calculated for $\langle p_\perp^2(z)\rangle$ is shown for Q = 15 and 30 GeV in fig. 16. The agreement with $\langle p_\perp^2(z)\rangle$ in sec. III is good, although the thrust cuts differ somewhat. (For completeness, we also present $\langle p_\perp^2(z)\rangle$ for Q = 90 GeV in fig. 17.) Finally, fig. (18) shows the Q dependence of the overall mean $\langle p_\perp^2\rangle$. Here again, the agreement with our earlier analytic results is satisfactory. We conclude that these features are acceptably clean tests of QCD.

The model can be employed to do other things as well. We have used it to consider the angular energy flow in $e^+e^- \to$ jets /20/. The idea is to calculate the average fraction of the CM energy, $F(Q,\delta)$, outside a cone of half opening angle δ about the thrust axis. We show the results from our $q\bar{q} + q\bar{q}G$ Monte Carlo model in Fig. (19). $F(Q,\delta)$ provides a global measure of jet broadening. This effect is not too dramatic at Q = 30 GeV, but is clearly substantial at Q = 90 GeV. We suspect that other calorimetric jet measures will show similar behavior.

Our last point is on the observability of true 3 jet structure, $e^+e^- \to q\bar{q}G \to$ 3 jets. Fig. (20) shows the angular energy pattern in the event plane /4/, [+)]

$$\frac{1}{E}\,\frac{dE_{\parallel}}{d\phi} \qquad (32)$$

[+)] note that both two and 3 jet events are included.

where the axes are chosen as the T' axis and the directions of the second and third most energetic quanta. (Here E is the total CM energy, and E_{11} is the projection in the $q\bar{q}G$ plane of the energy at azimuth ϕ) Three jet structure is clearly evident even at 15 GeV CM energy. (Of course, this will be obscured somewhat in practice by $e^+e^- \rightarrow b\bar{b} \rightarrow$ hadrons.)

Since this model may be of use to experimentalists, we close this section with a note on its respectability. At not too high energies (Q above 70 or 90 GeV) this is not so. This is because of the way we have enforced conservation of probability. We simply set $\sigma_{2jet} + \sigma_{3jet} = (1+\frac{\alpha}{\pi})\sigma_0$ This clearly cannot work once $\sigma_{3jet} > \sigma_0$. It is then necessary to take higher orders in α_s into account. Intuitively it is clear that then a four jet cross section will appear, and σ_{2jet} will be damped less strongly than given by (31). A precise and physically acceptable way of doing this is not yet available. (Of course, neither are the e^+e^- CM energies where this is certain to be relevant.)

V. Summary and Remarks

Our aim has been to find convincing tests of QCD jet broadening in e^+e^- annihilation. In particular, we observe that before 3 jets become easily visible, one jet in $e^+e^- \rightarrow$ 2 jets broadens and the other does not. This effect can be predicted quantitatively for energies of 30 GeV and above. If no new flavor thresholds intervene, this must be observed. It is present below 30 GeV, but quantitative predictions appear more uncertain . Tests that jet broadening is due to the radiation of vector quanta without flavor are

also feasible. But they appear less simple than a check of jet broadening itself.

In the course of verifying that we can make quantitative predictions, we have developed a Monte Carlo multijet model for $e^+e^- \rightarrow q\bar{q} + q\bar{q}G \rightarrow$ jets. Subject to our cautionary remarks on the completeness of the model, we hope that experimentalists can use it. It provides a useful explicit account of QCD effects at not too high energies. This may be especially helpful if it becomes necessary to separate QCD effects in the complicated final states above a new heavy flavor threshold.

Acknowledgements

We want to thank members of the PLUTO and TASSO groups for discussions, and G. Schierholz for comments on scalar gluon angular distributions.

References

1) A.M. Polyakov, JETP 32 (1971) 296; 33 (1971) 850

2) H. Politzer, Phys. Rev. Lett. 30 (1973) 1346
D.J. Gross and F. Wilczek, Phys. Rev. D8 (1973) 3497
H. Politzer, Phys. Reports 14C (1974) 129
H. Politzer, Phys. Lett. 70B (1977) 430

3) J. Ellis, M.K. Gaillard and G. Ross, Nucl. Phys. B111 (1976) 253
T. DeGrand, Y.J. Ng and S.-H. Tye, Phys. Rev. D16 (1977) 3251

4) A. De Rujula et al., Nucl. Phys. B138 (1978) 387
E. Farhi, Phys. Rev. Lett. 39 (1977) 1587
S. Brandt et al., Phys. Lett. 12 (1964) 57

5) G.C. Fox and S. Wolfram, Nucl. Phys. B149 (1979) 413

6) S.Y. Pi, R.L. Jaffe and F. Low, Phys. Rev. Lett. 41 (1978) 142

7) G. Kramer, G. Schierholz and J. Willrodt, Phys. Lett. 79B (1978) 249;
erratum 80B (1979) 433

8) A. Ali et al., DESY 79/03 (January, 1979)

9) J. Ellis and I. Karliner, Nucl. Phys. B148 (1979) 141

10) A. Ali et al., papers in preparation

11) R. Field and R.P. Feynman, Nucl. Phys. B136 (1978) 1

12) B. Andersson, G. Gustafson and C. Peterson, Nucl. Phys. B135 (1978) 273

13) H. Georgi and M. Machacek, Phys. Rev. Lett. 39 (1977) 1237
H. Georgi and J. Sheiman, HUTP-78/A034

14) G. Sterman and S. Weinberg, Phys. Rev. Lett. 39 (1977) 1436

15) T. Kinoshita, J. Math. Phys. 3 (1962) 650
T.D. Lee and M. Nauenberg, Phys. Rev. 133 (1964) B1549

16) G. Hanson, SLAC-LBL-2119 (May, 1978)

17) G. Kramer and G. Schierholz, Phys. Lett. 82B (1979) 108

18) K. Koller and T.F. Walsh, Phys. Lett. 72B (1977) 227

19) L. Sehgal, 1977 Lepton-Photon Symposium (ed. F. Gutbrod, Hamburg 1978)

20) Ch. Berger et al., Phys. Lett. 78B (1978) 176
F. Steiner, DESY 78/59 (October 1978)
I. Bigi and T.F. Walsh, DESY 78/72 (November, 1978)

21) T.F. Walsh and P. Zerwas, Nucl. Phys. B77 (1974) 494

Figure Captions

Fig. 1. Gluon bremsstrahlung, $e^+e^- \rightarrow q\bar{q}G$

Fig. 2. $q\bar{q}G$ kinematics

Fig. 3. Plot of $\frac{1}{\sigma}\frac{d\sigma}{dx_\perp}$ where $x_\perp = \frac{1}{2}\sum_i |p_\perp^i| / E_B$.

Fig. 4. Plot of the average $\langle x_\perp^n \rangle$ versus the minimum $x_\perp^{min}$.

Fig. 5. The charge correlation $C(T)/C(1)$.

Fig. 6. The cross sections $d\sigma^i$, $i = U, L, I$ for vector and scalar gluons (solid and dashed lines).

Fig. 7. The average $\langle p_\perp^2 \rangle / \langle p_\perp^2 \rangle_{NP}$ and $\langle p_\perp^4 \rangle / \langle p_\perp^4 \rangle_{NP}$ including gluon bremsstrahlung.

Fig. 8a. The profile function G(z) for several choices of D_q and D_G from refs. /18/ and /19/.

Fig. 8b. The profile G(z) for vector and scalar gluons, $D_G = D_q \propto z^{-1}(1-z)^2$.

Fig. 9. The dependence of G(z) on the cutoff T_o.

Fig. 10. The asymmetry in $\langle p_\perp^2(z) \rangle$. The narrow (non perturbative) jet is on the left. The right jet is broadened by gluon radiation.

Fig. 11. Plot of $\langle P_\perp^2(z;T)\rangle/Q^2$ for various thrust regions.

Fig. 12. $\langle P_\perp^2(T)\rangle / Q^2$ averaged over z as a function of thrust T.

Fig. 13a. The π^+/π^- ratio given a high momentum π^+ ($z \geq .8$) on the opposite side. Various values of T are shown.

Fig. 13b. The same as above, but for $q\bar{q}$ jets only. The difference of 13a and 13b shows the effect of gluon bremsstrahlung.

Fig. 14. $(1/\sigma)\, d\sigma/dT$ for $e^+e^- \rightarrow q\bar{q} \rightarrow$ 2 jets, from our Monte Carlo model.

Fig. 15. $(1/\sigma)\, d\sigma/dT$ for $e^+e^- \rightarrow q\bar{q} + e^+e^- \rightarrow q\bar{q}G, \rightarrow$ jets, from our Monte Carlo model.

Fig. 16. The asymmetry in $\langle P_\perp^2(z)\rangle$ from our $q\bar{q} + q\bar{q}G \rightarrow$ jets Monte Carlo model. This figure should be compared to Fig. 10.

Fig. 17. The asymmetry $\langle P_\perp^2(z)\rangle$ for 90 GeV CM energy.

Fig. 18. $\langle P_\perp^2\rangle$ as a function of the CM energy from our Monte Carlo model.

Fig. 19. The energy flow $F(Q,\delta)$ at 30 and 90 GeV CM energy. We show non-perturbative $q\bar{q}$ jets as well as the full $q\bar{q} + q\bar{q}G$ result from our Monte Carlo model.

Fig. 20. The energy flux pattern in the event plane of e^+e^- → jets, at energies of 15, 30 and 90 GeV.

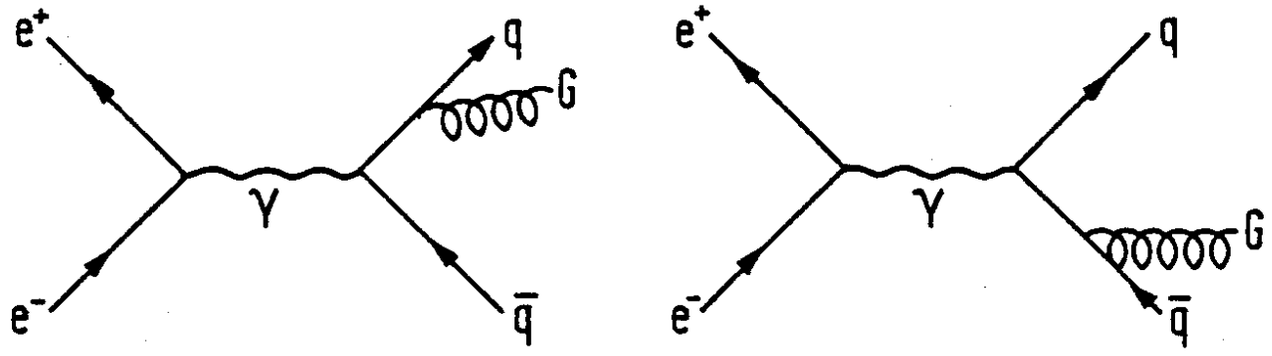

Fig.1

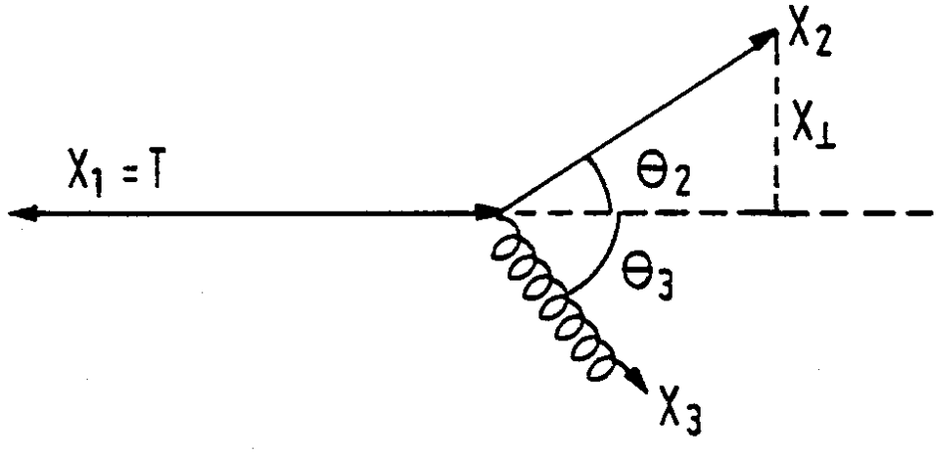

Fig.2

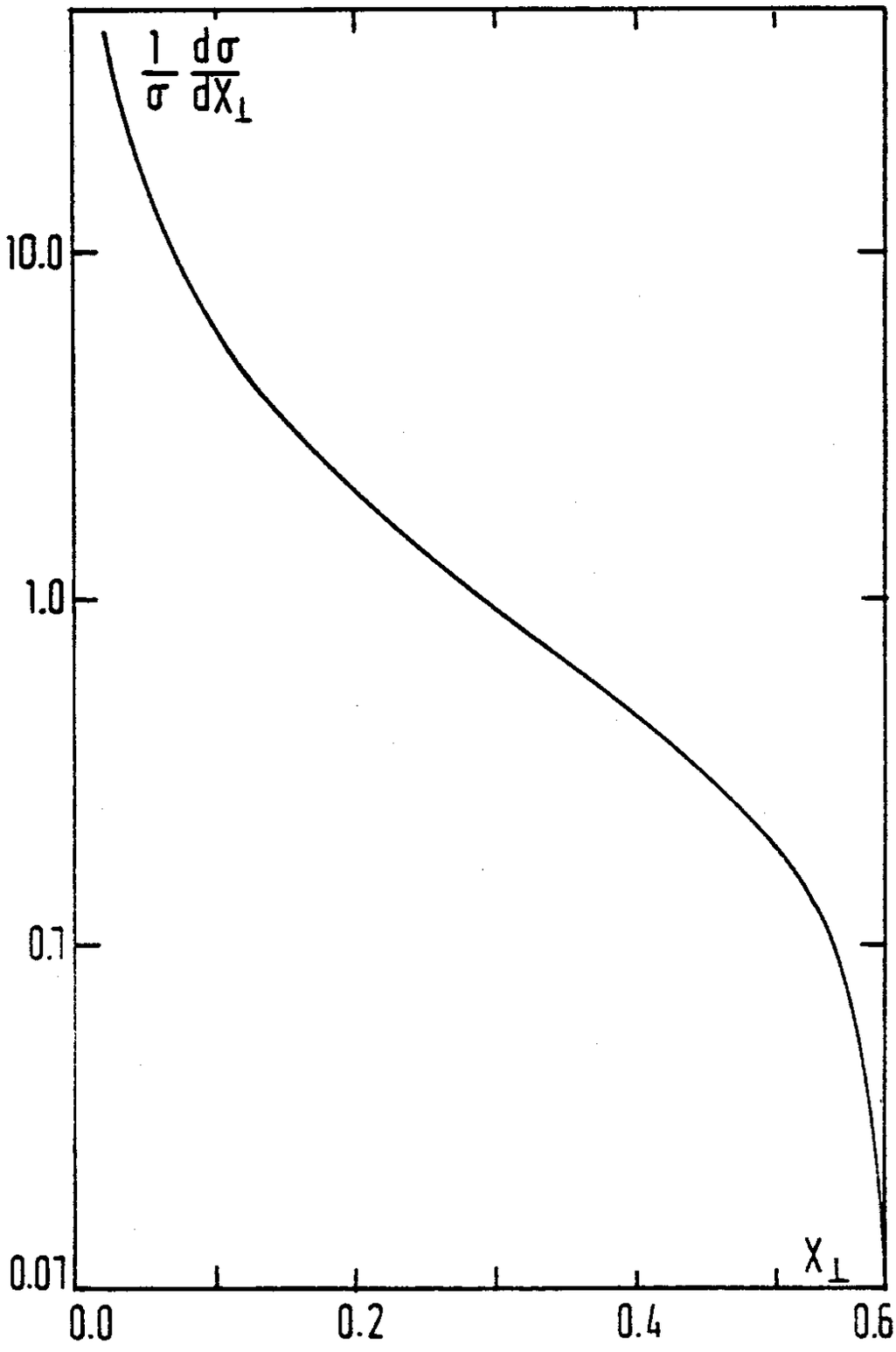

Fig.3

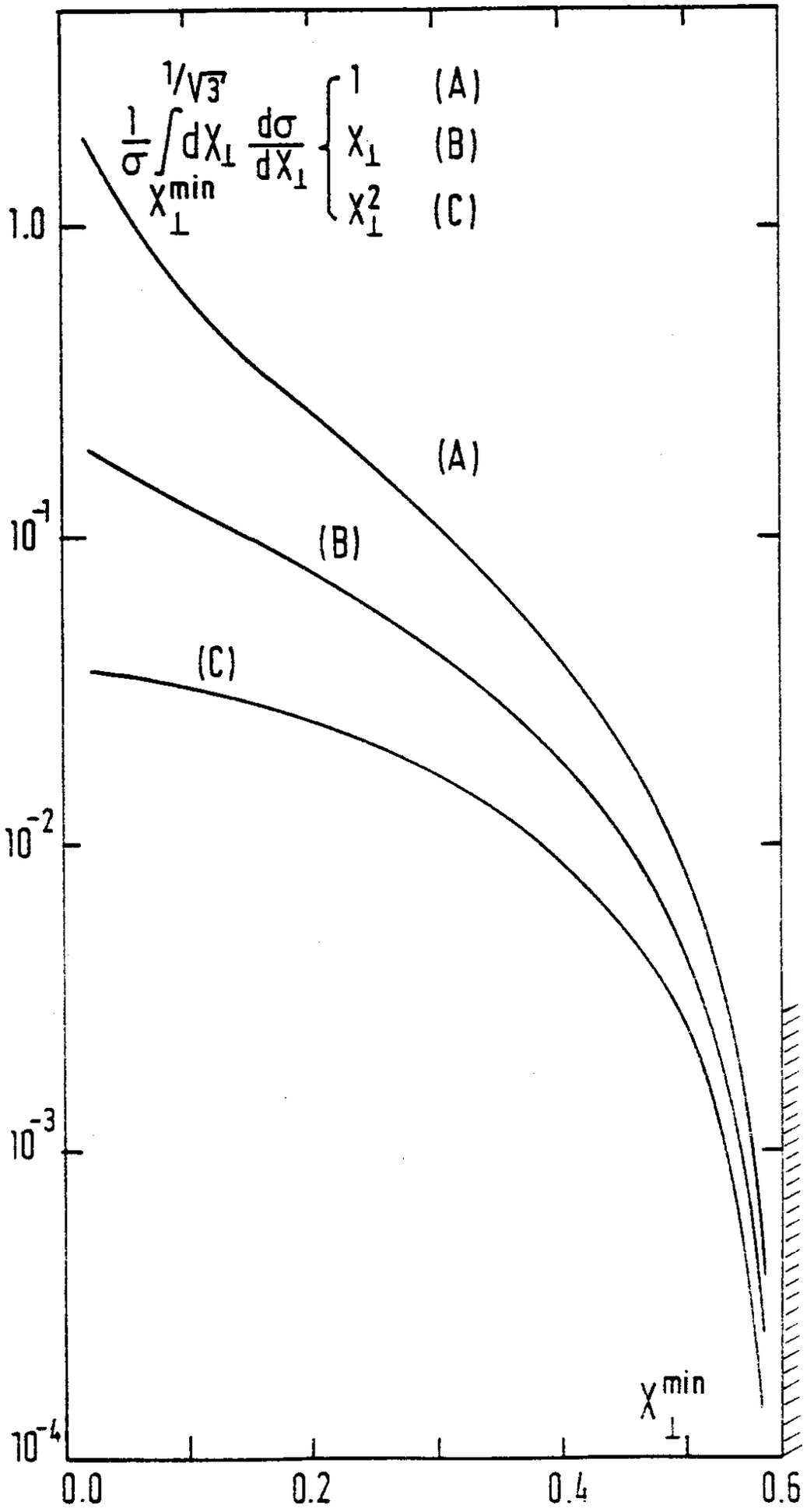
$\frac{1}{\sigma}\int_{X_\perp^{min}}^{1/\sqrt{3}} dX_\perp \frac{d\sigma}{dX_\perp}\begin{cases}1 & (A)\\ X_\perp & (B)\\ X_\perp^2 & (C)\end{cases}$
1.0
10^{-1}
10^{-2}
10^{-3}
10^{-4}
(A)
(B)
(C)
$X_\perp^{min}$
0.0
0.2
0.4
0.6

Fig. 4

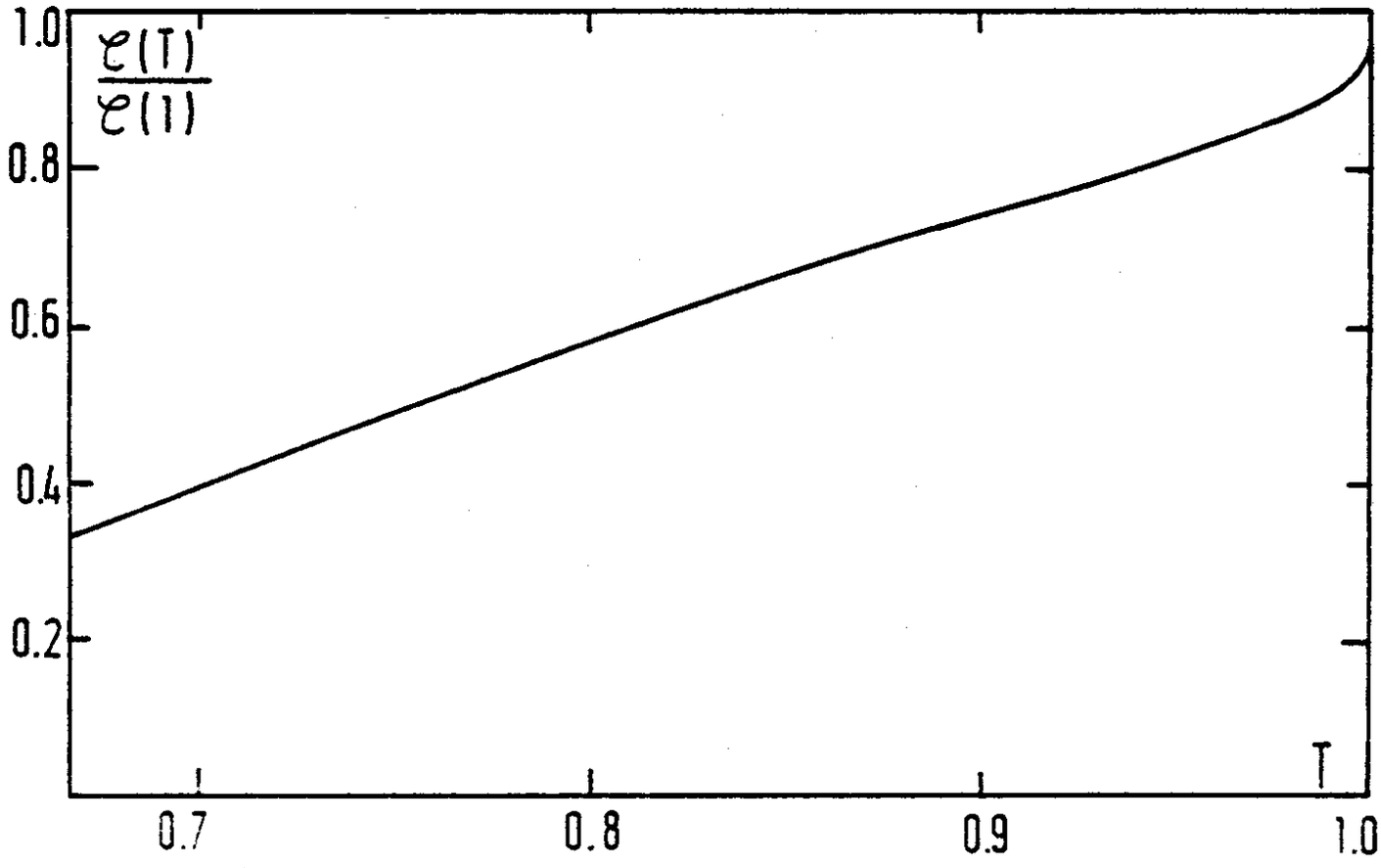

Fig.5

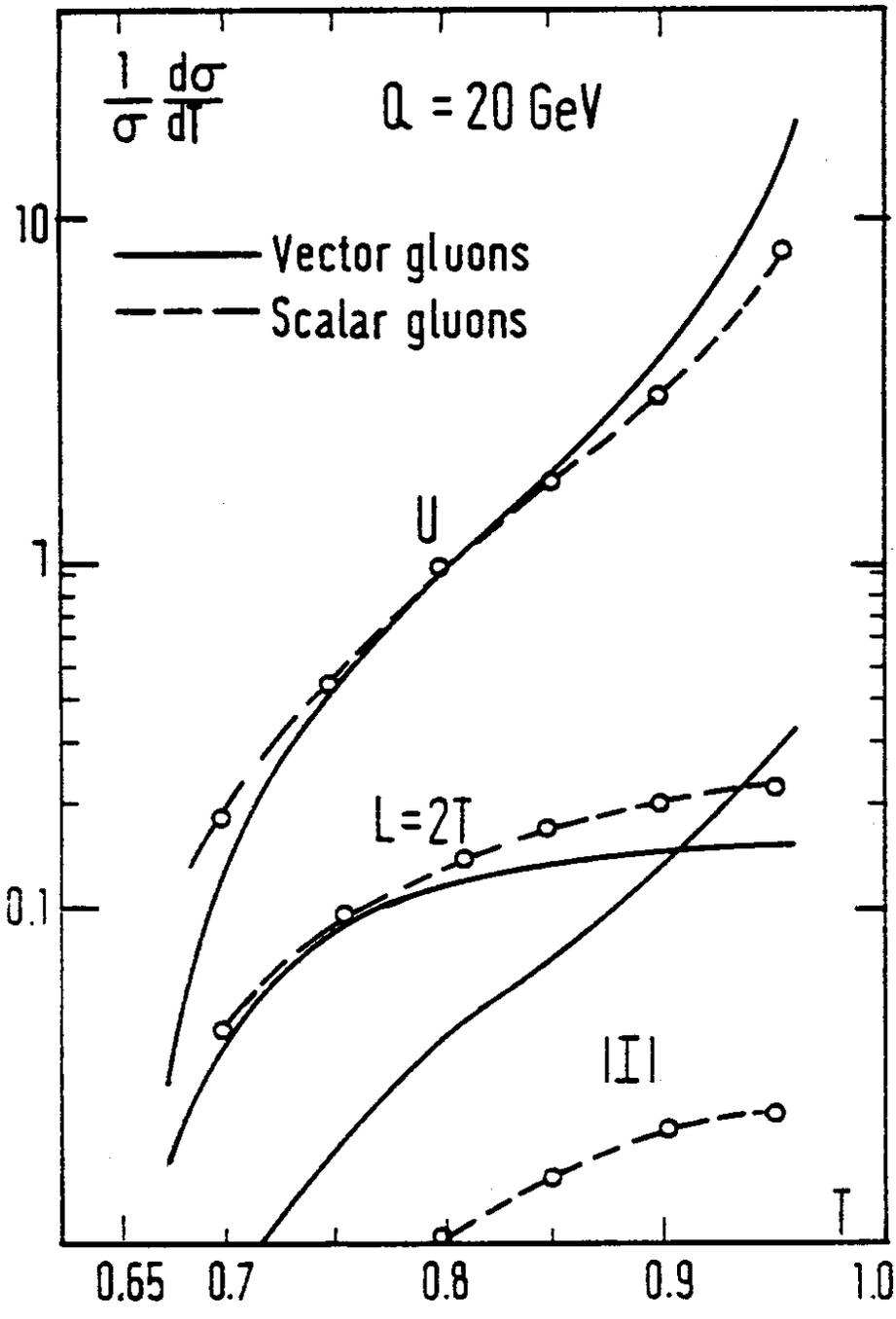
$\frac{1}{\sigma}\frac{d\sigma}{dT}$
Q = 20 GeV
10
1
0.1
Vector gluons
Scalar gluons
U
L=2T
|I|
T
0.65
0.7
0.8
0.9
1.0

Fig.6

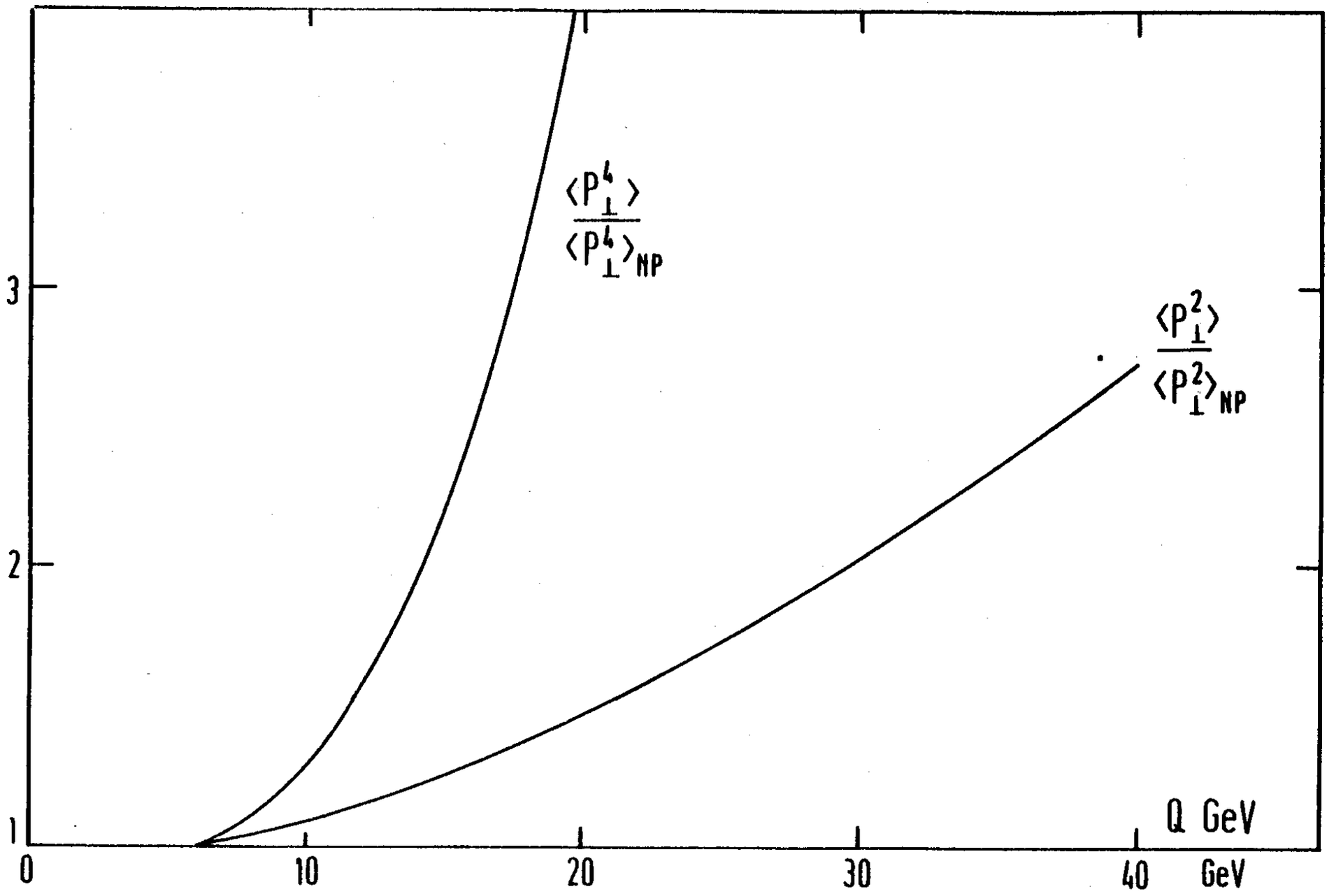
$\frac{\langle P_\perp^4 \rangle}{\langle P_\perp^4 \rangle_{NP}}$
$\frac{\langle P_\perp^2 \rangle}{\langle P_\perp^2 \rangle_{NP}}$
3
2
1
0
10
20
30
40
GeV
Q GeV

Fig.7

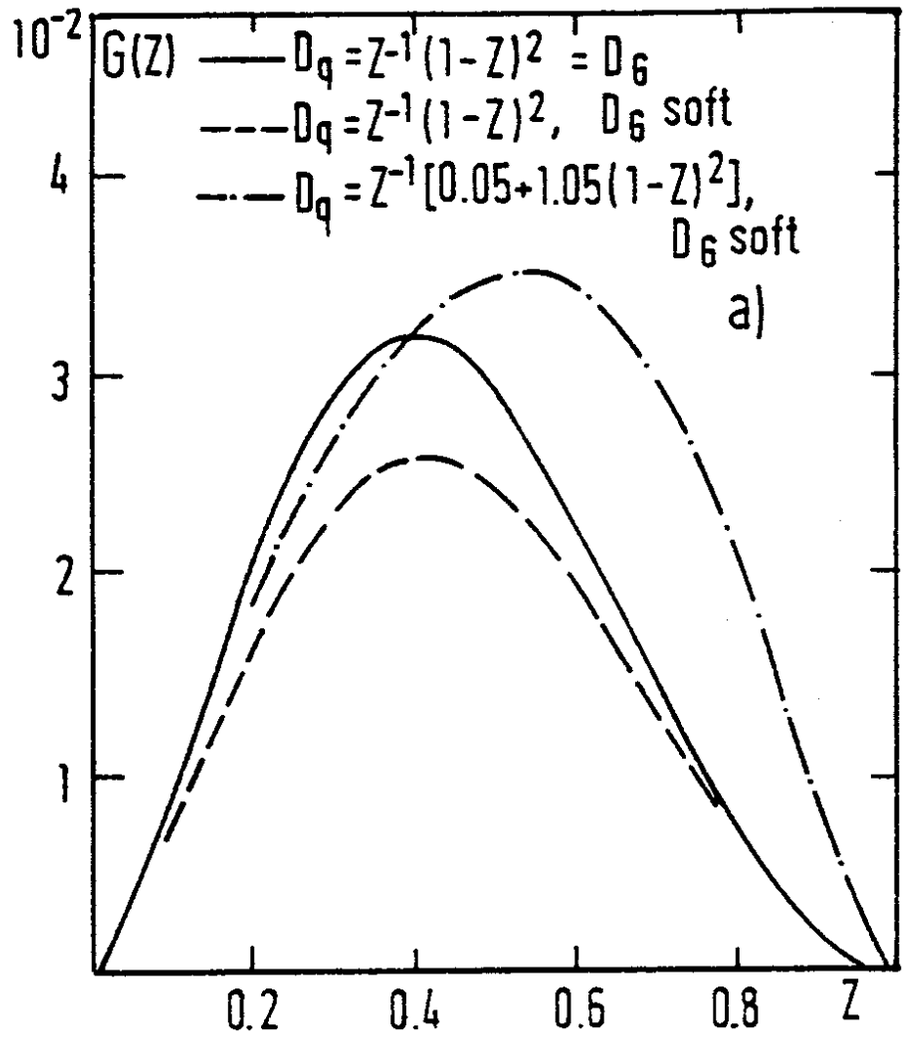
10^{-2}
G(Z)
$D_q = Z^{-1}(1-Z)^2 = D_6$
$D_q = Z^{-1}(1-Z)^2$, D_6 soft
$D_q = Z^{-1}[0.05+1.05(1-Z)^2]$, D_6 soft
a)
4
3
2
1
0.2
0.4
0.6
0.8
Z

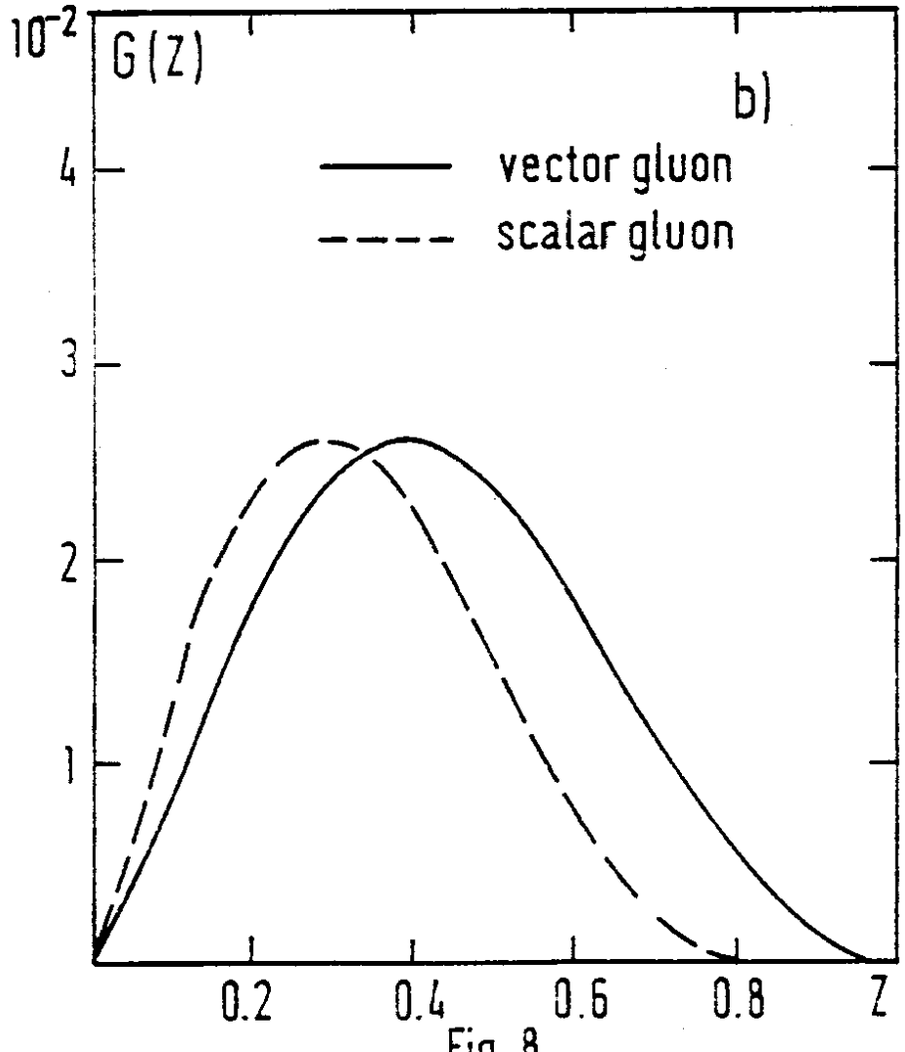
10^{-2}
G(Z)
b)
vector gluon
scalar gluon
4
3
2
1
0.2
0.4
0.6
0.8
Z

Fig. 8

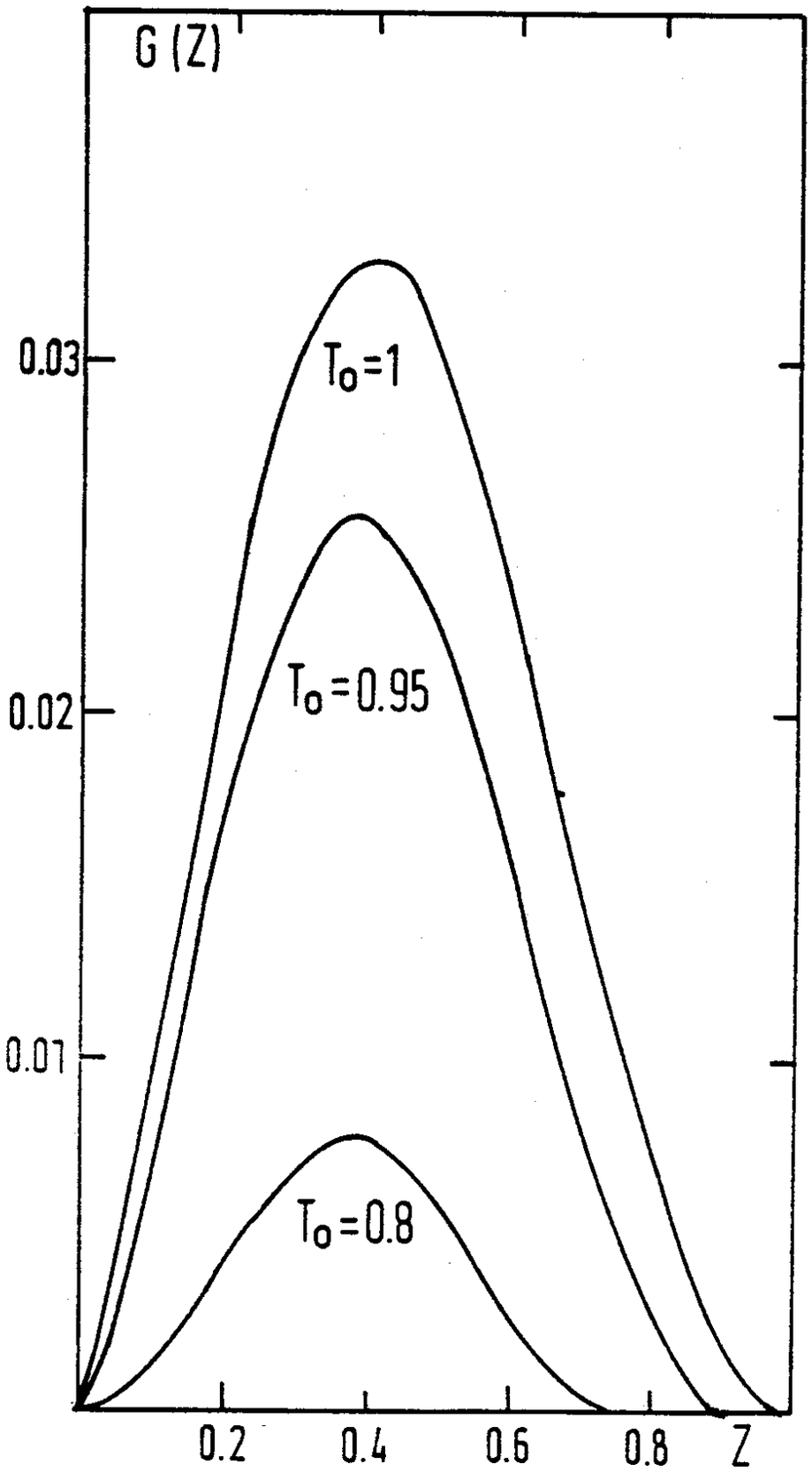

Fig.9

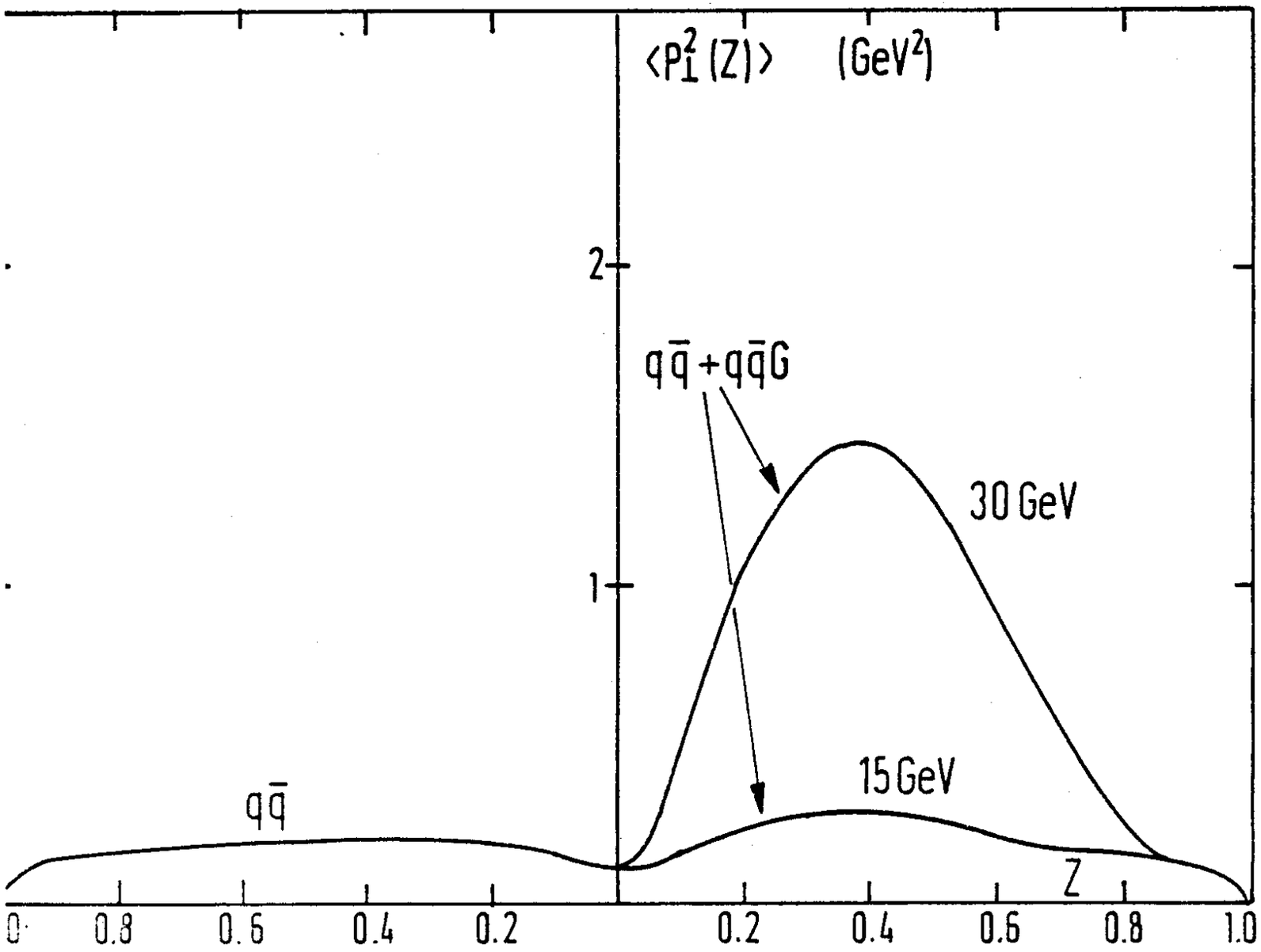
$\langle P_\perp^2(Z)\rangle$ (GeV^2)
2
1
$q\bar{q}+q\bar{q}G$
30 GeV
15 GeV
$q\bar{q}$
Z
0
0.8
0.6
0.4
0.2
0.2
0.4
0.6
0.8
1.0

Fig. 10

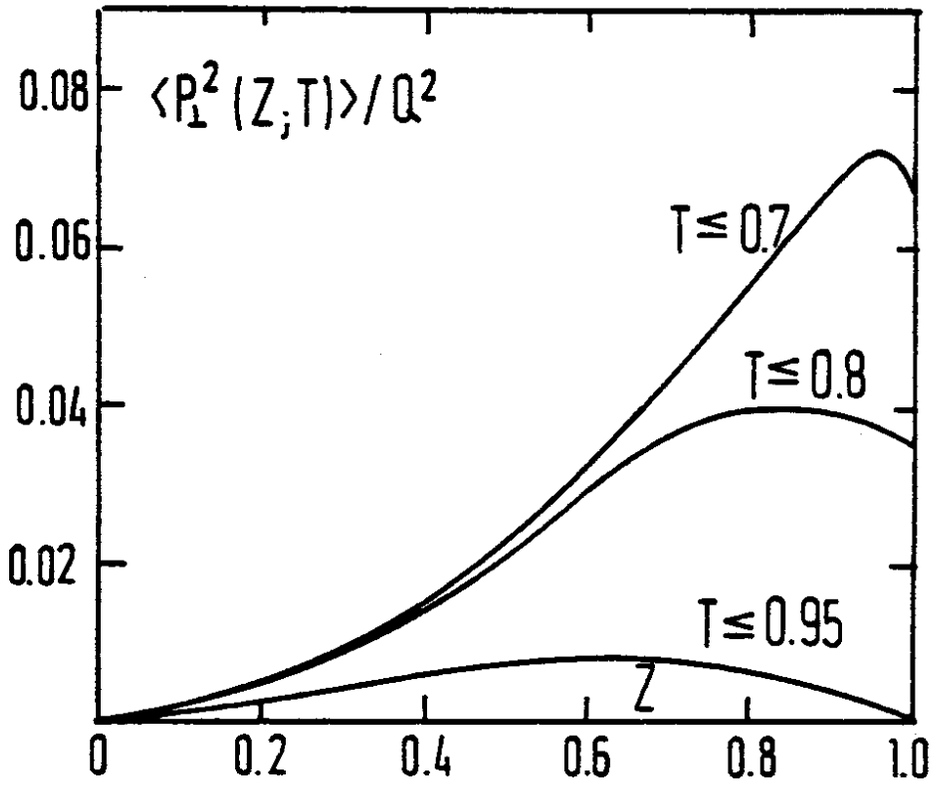
$\langle P_\perp^2(Z;T)\rangle/Q^2$
0.08
0.06
0.04
0.02
T≤0.7
T≤0.8
T≤0.95
Z
0
0.2
0.4
0.6
0.8
1.0

Fig.11

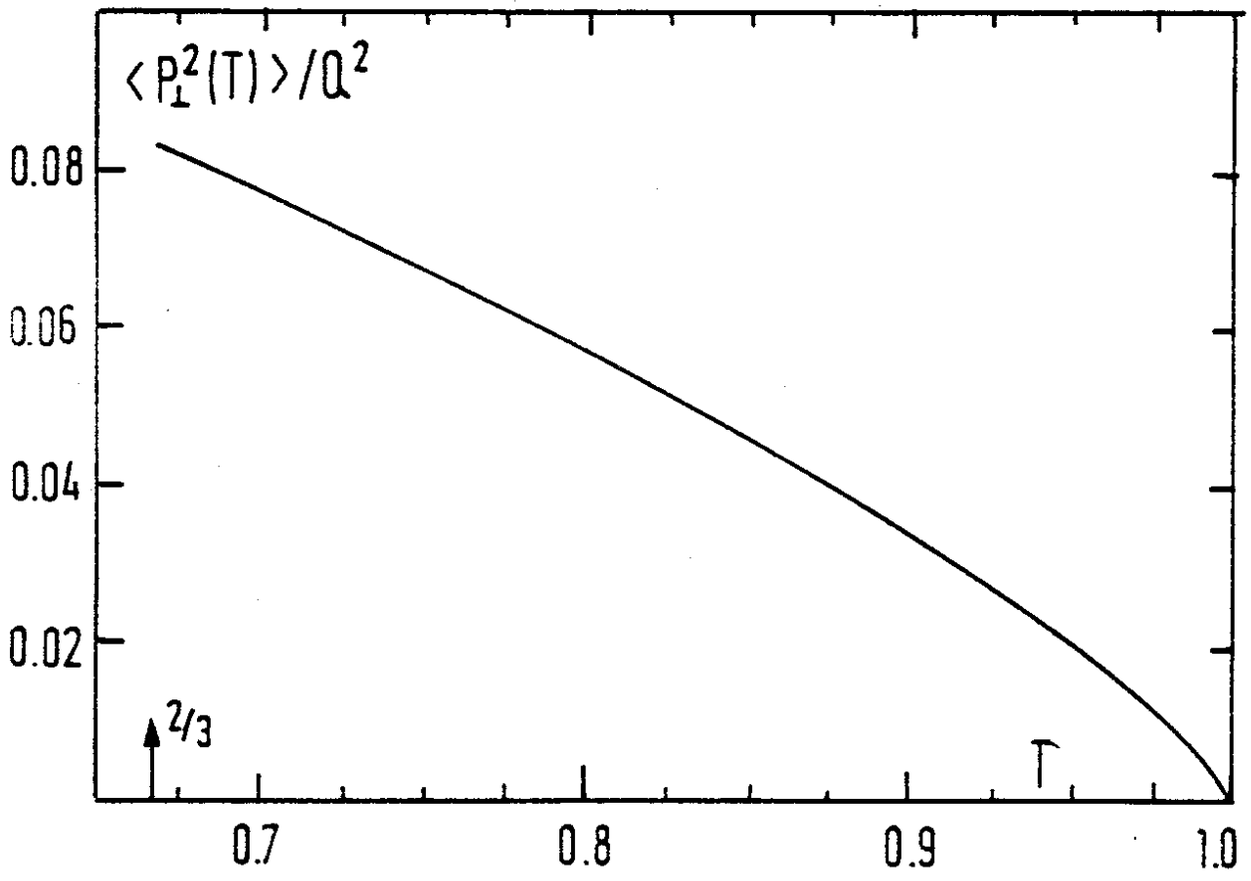
$\langle P_\perp^2(T)\rangle/Q^2$
0.08
0.06
0.04
0.02
2/3
T
0.7
0.8
0.9
1.0

Fig.12

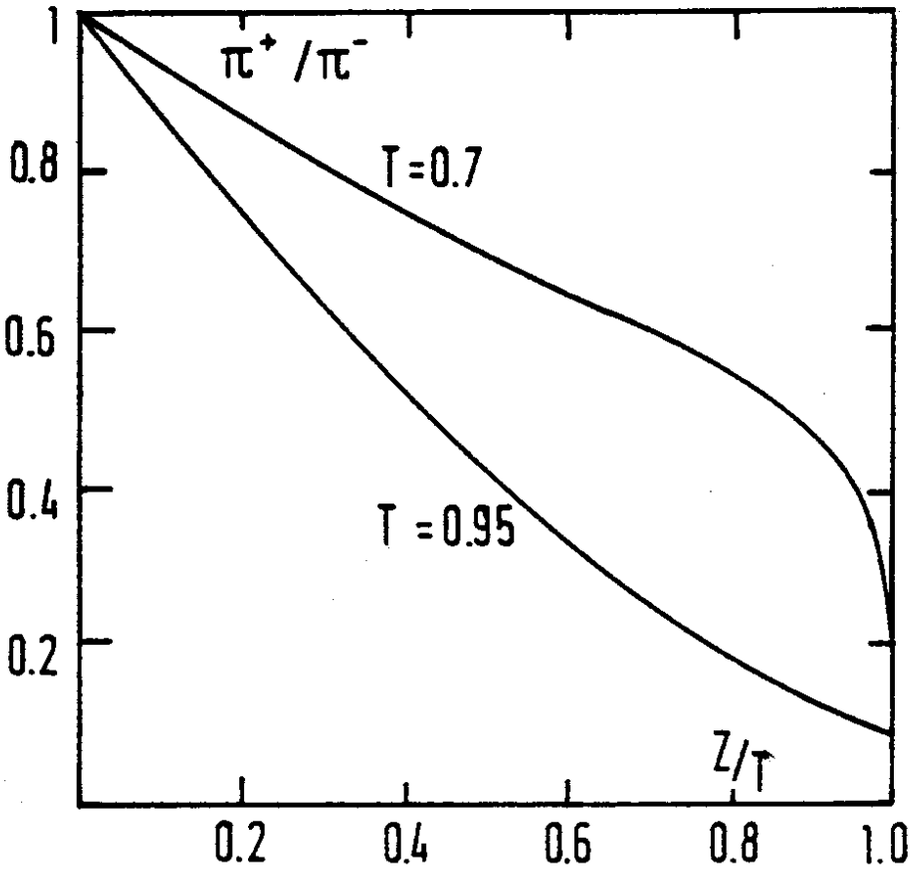

Fig. 13a

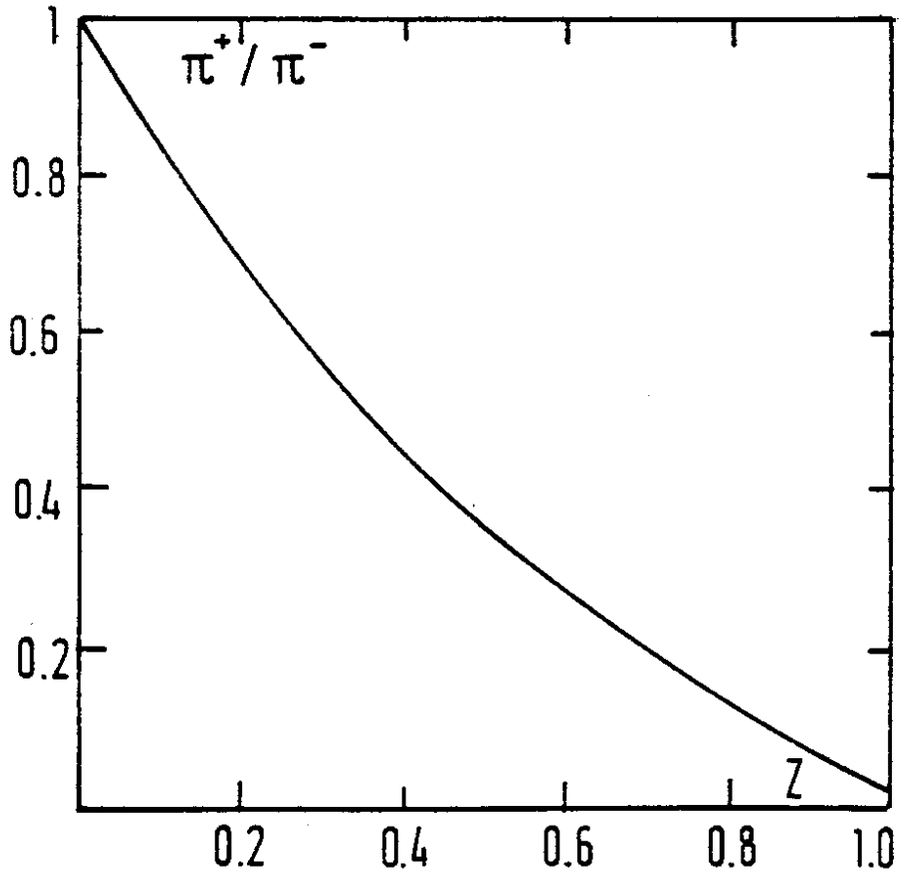

Fig. 13 b

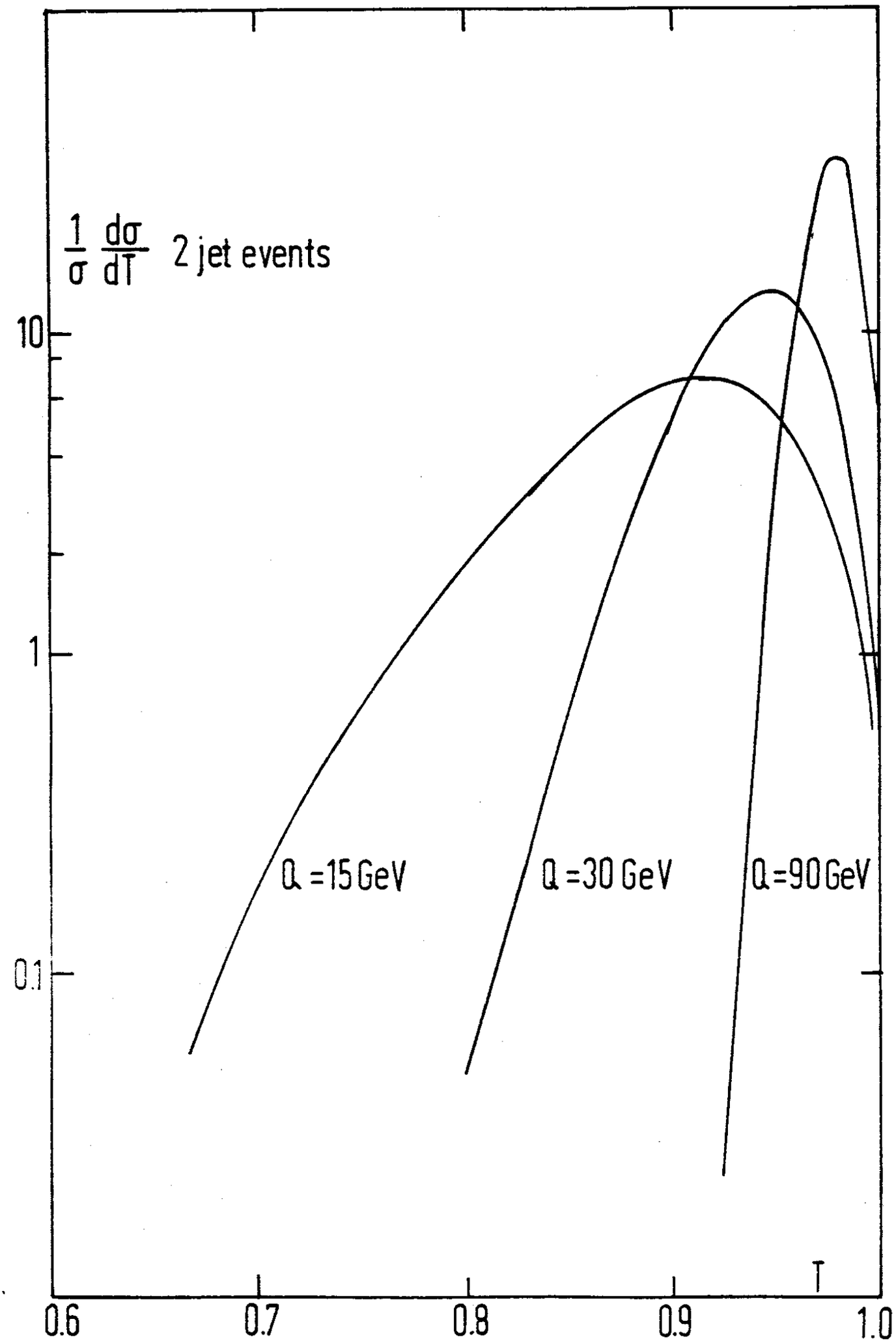
$\frac{1}{\sigma}\frac{d\sigma}{dT}$ 2 jet events
10
1
0.1
Q = 15 GeV
Q = 30 GeV
Q = 90 GeV
T
0.6
0.7
0.8
0.9
1.0

Fig. 14

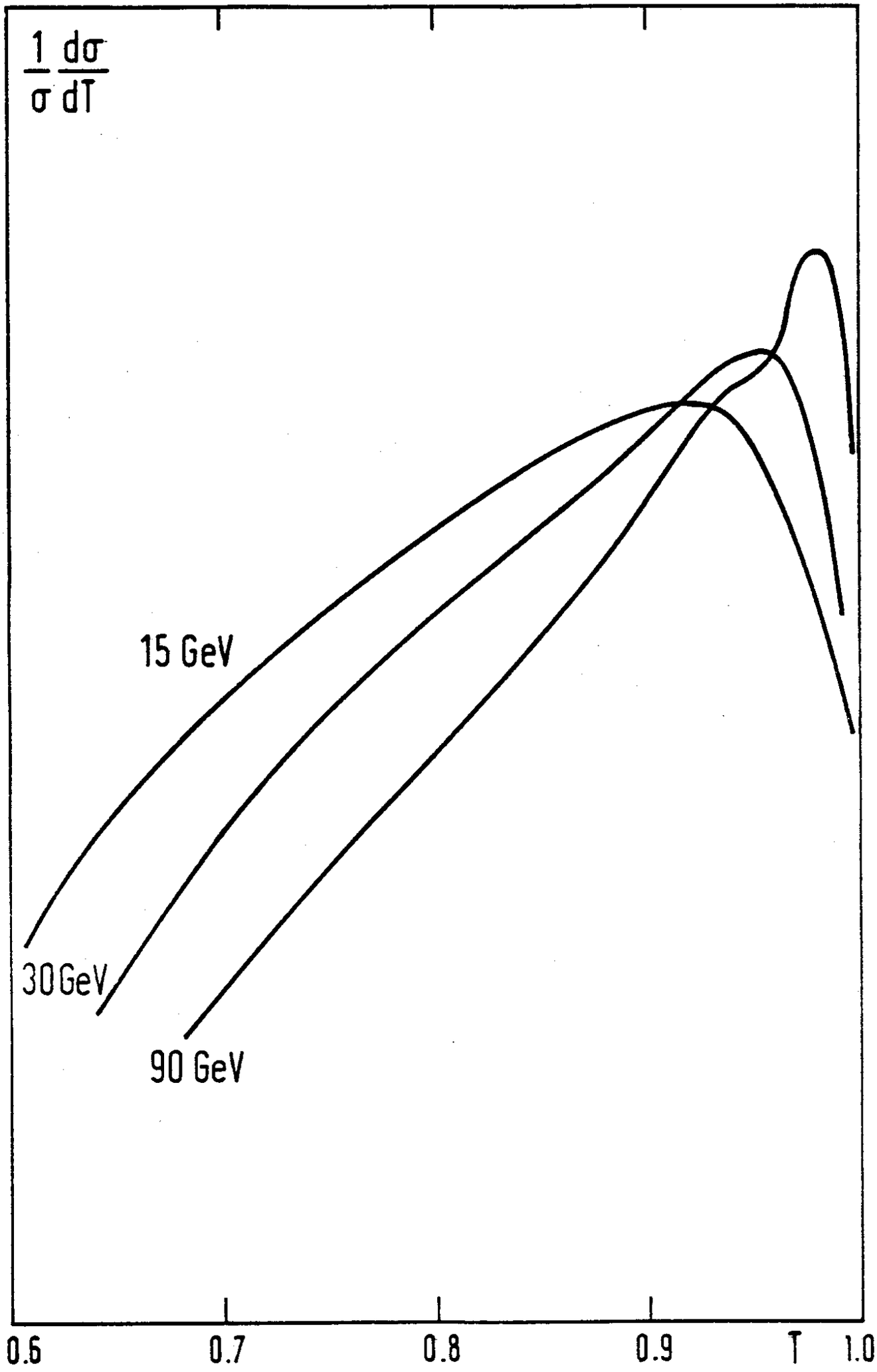

Fig. 15

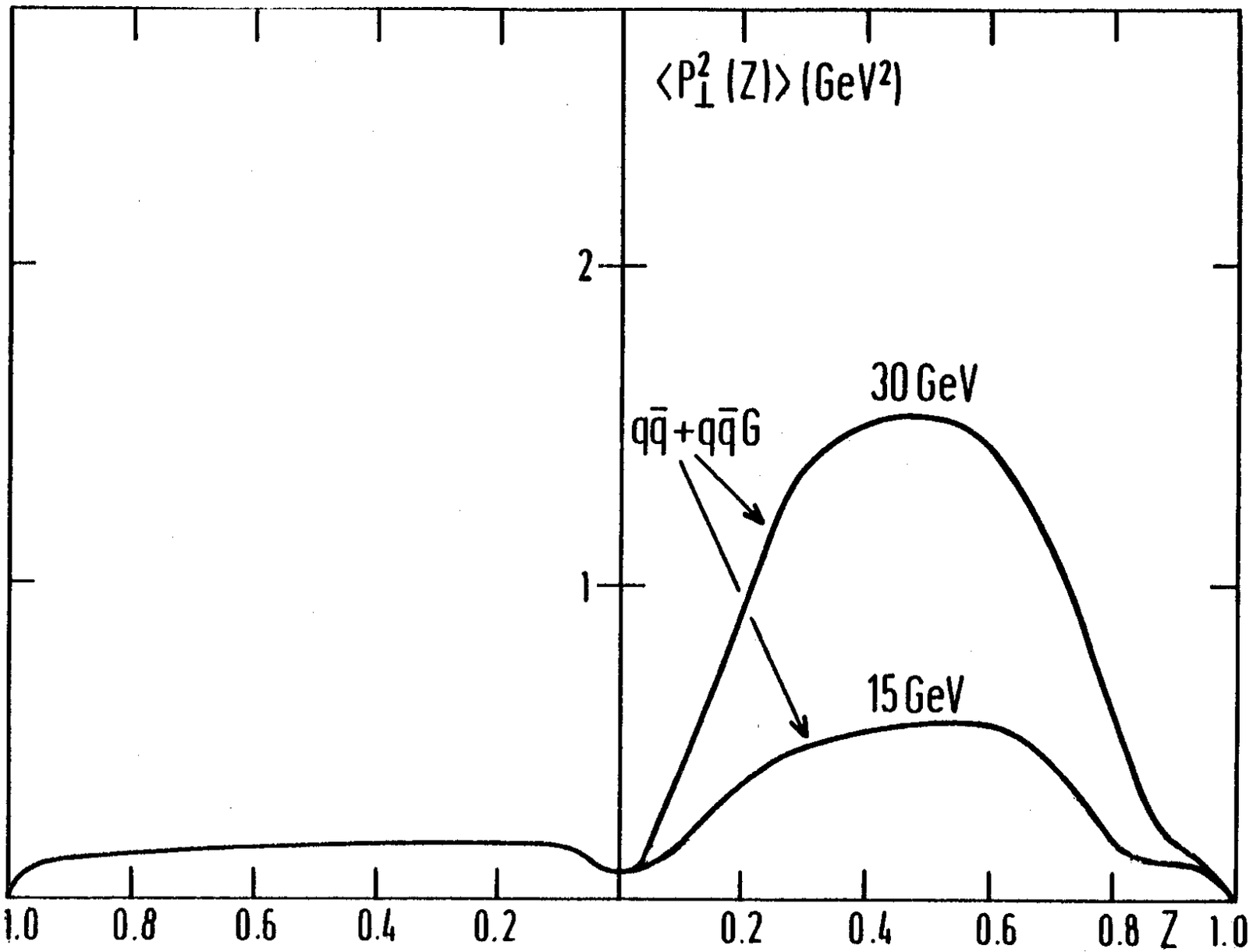
$\langle P_\perp^2(Z)\rangle$ (GeV²)
2
1
30 GeV
$q\bar{q}+q\bar{q}G$
15 GeV
1.0
0.8
0.6
0.4
0.2
0.2
0.4
0.6
0.8
Z
1.0

Fig.16

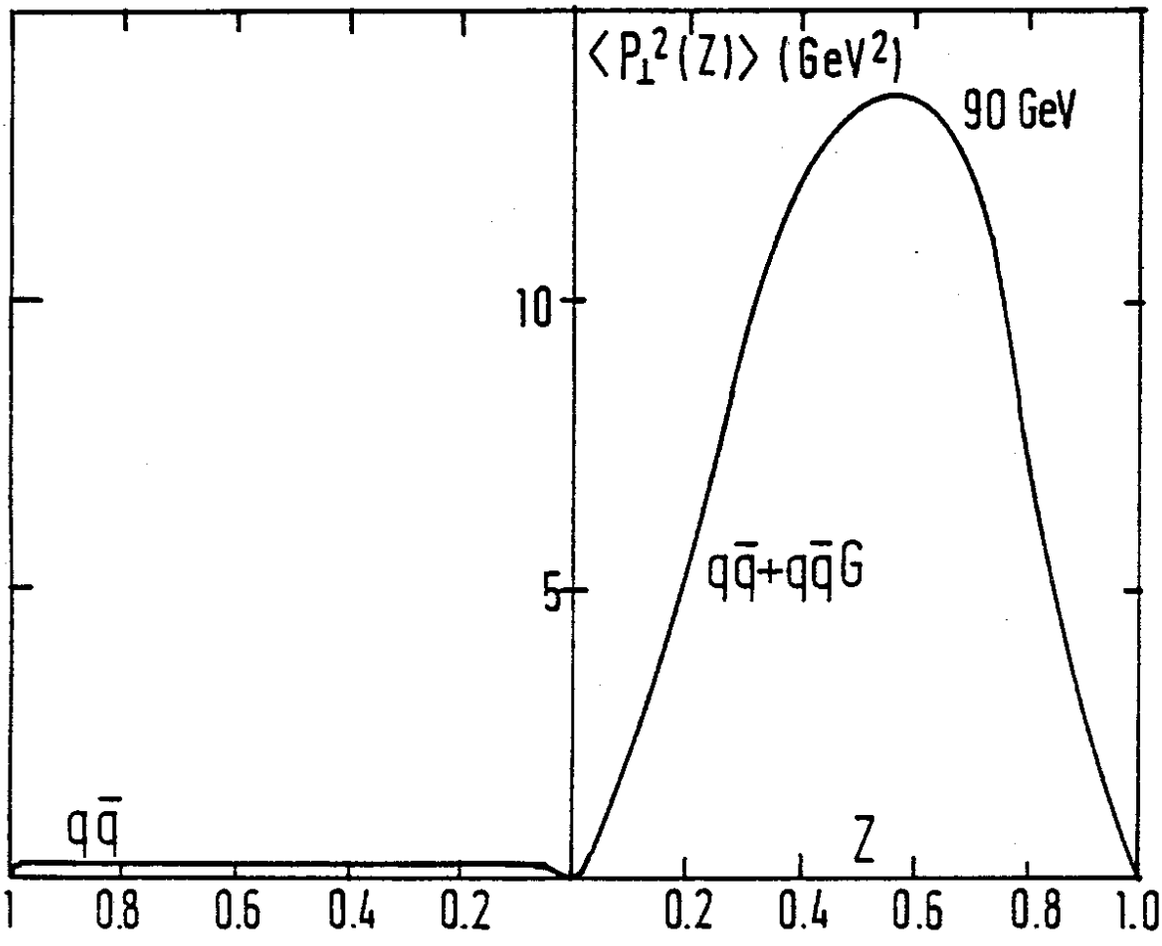

Fig.17

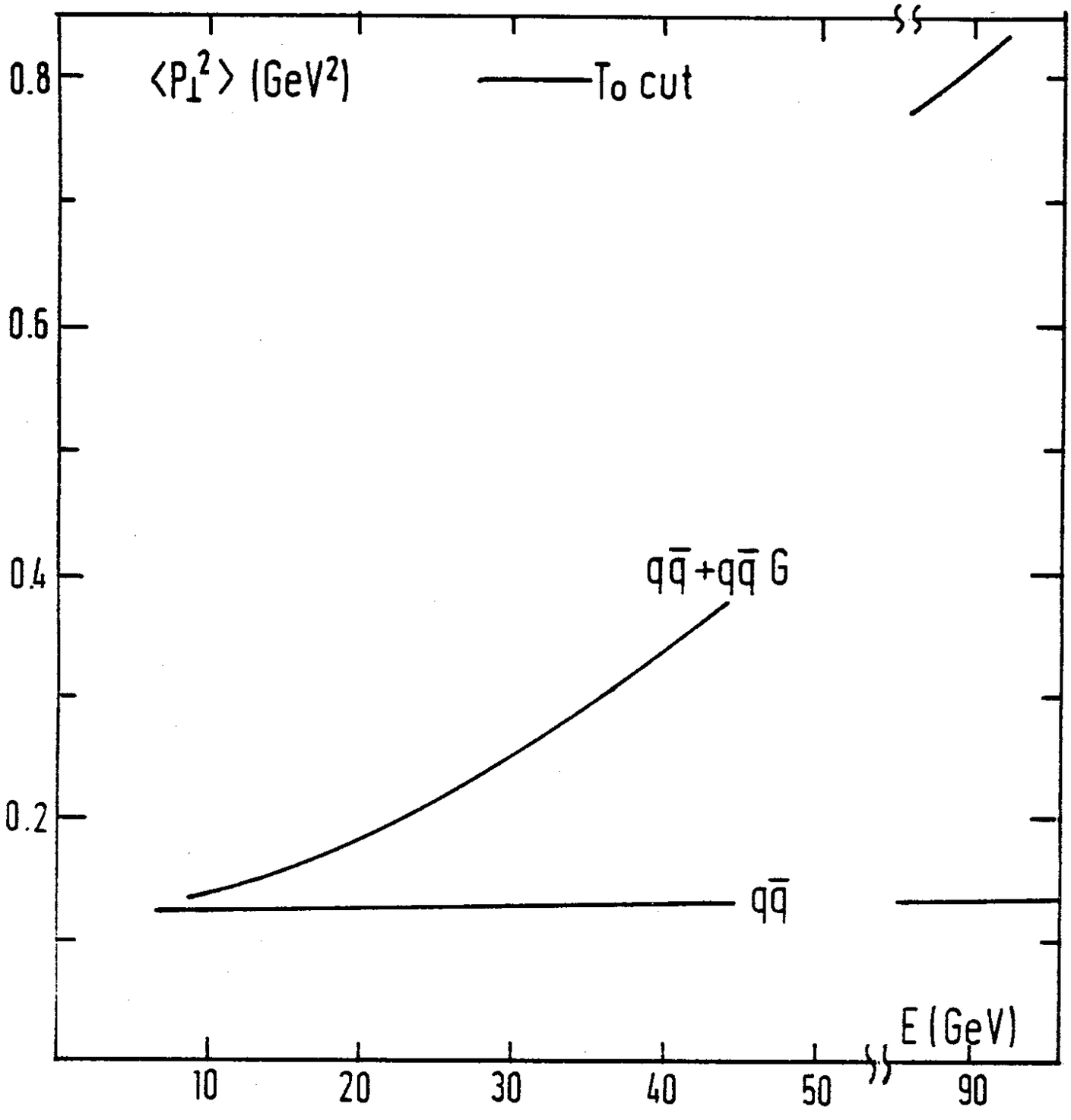
0.8
0.6
0.4
0.2
$\langle P_\perp^2 \rangle$ (GeV^2)
—— T_o cut
$q\bar{q}+q\bar{q}G$
$q\bar{q}$
E (GeV)
10
20
30
40
50
90

Fig. 18

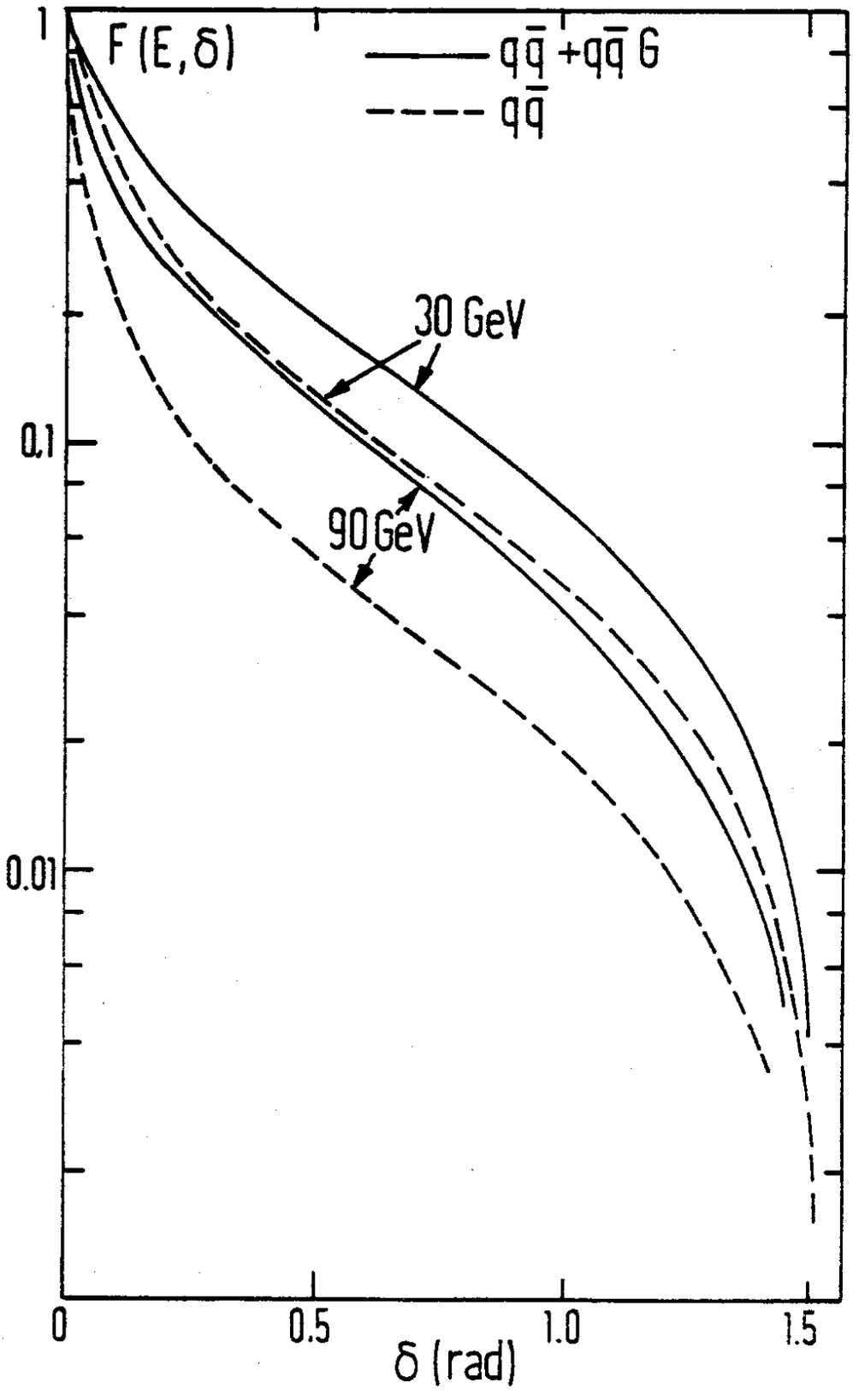

Fig. 19

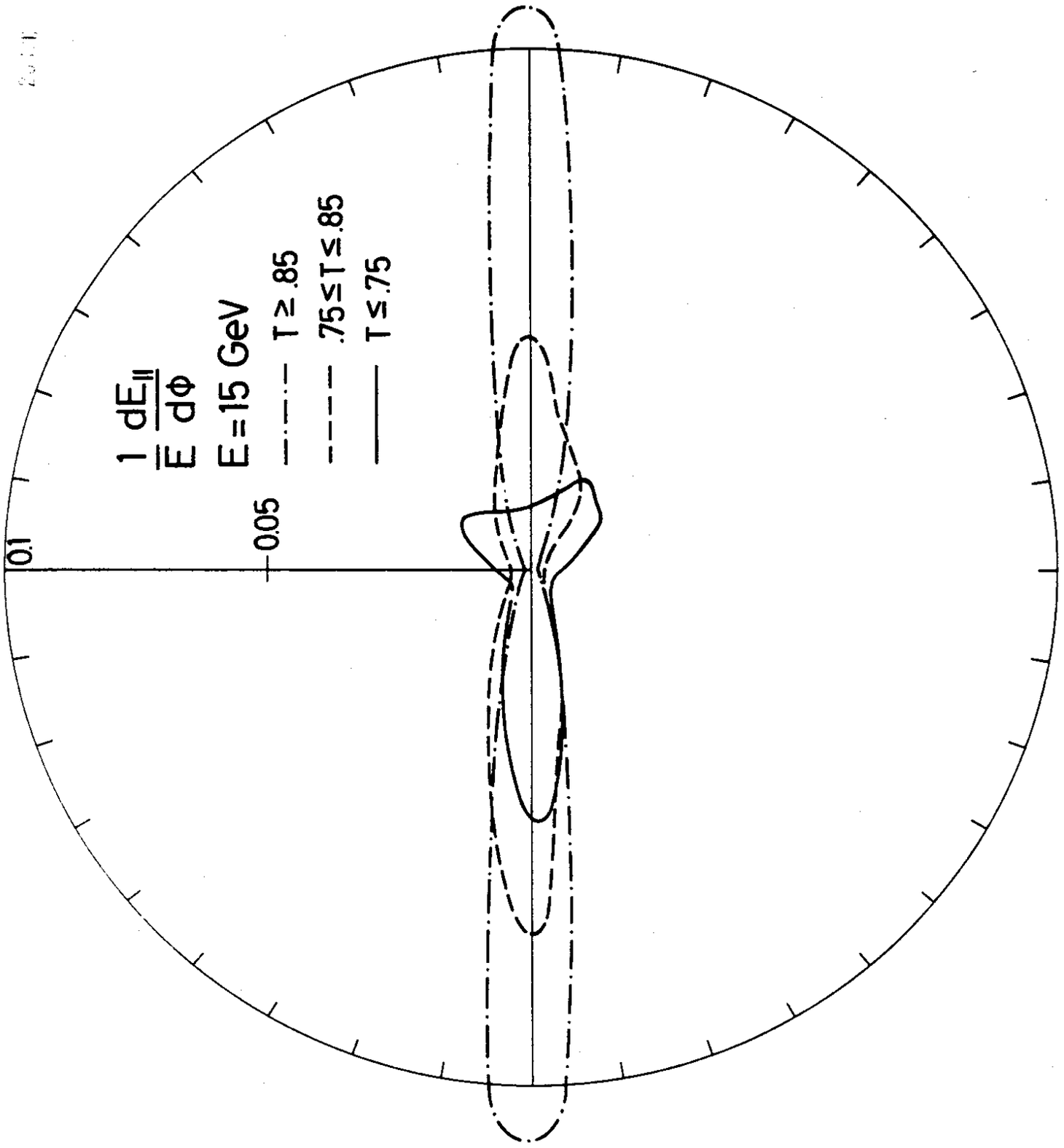

fig. 20a

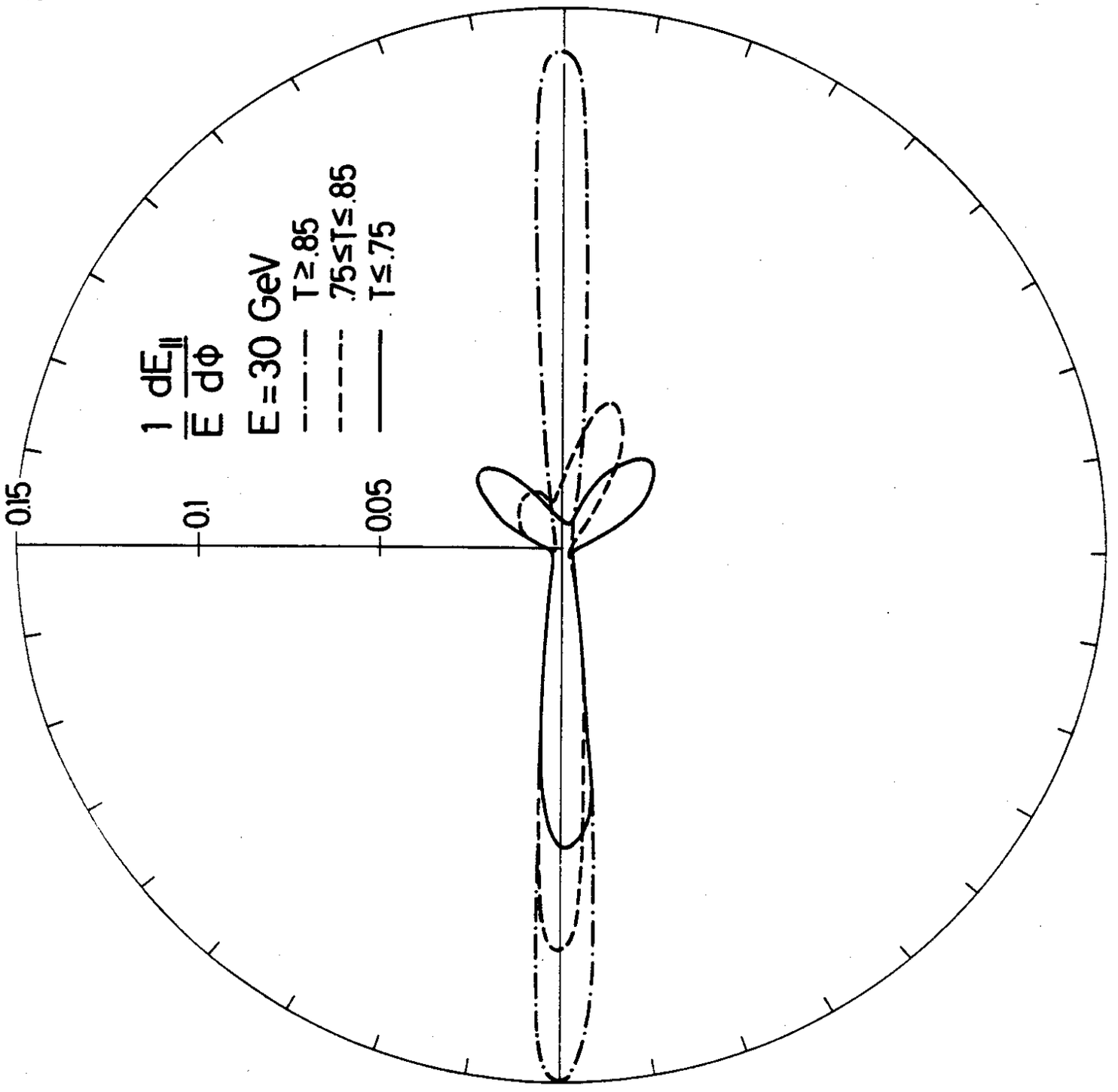

fig. 20b

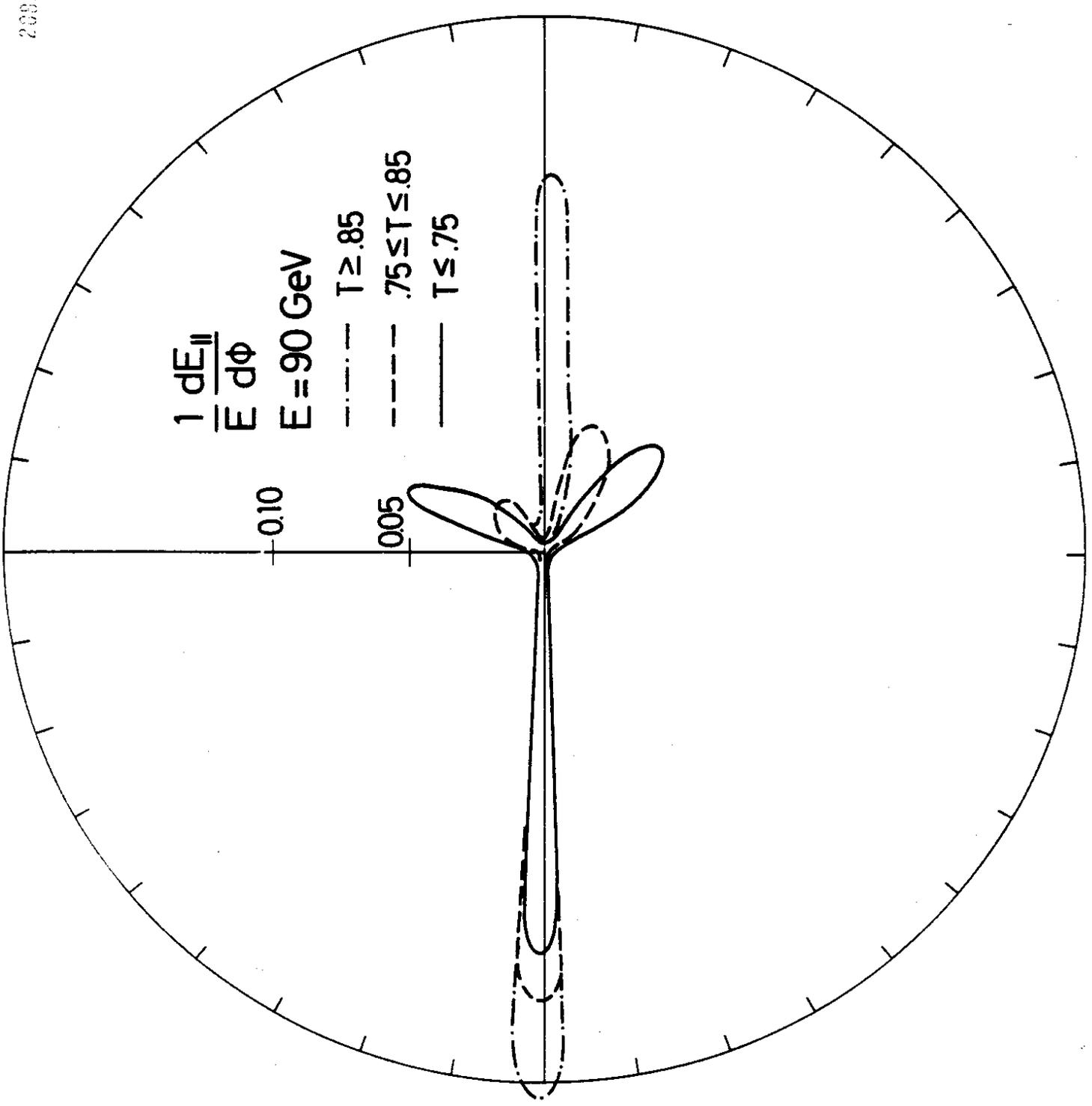

fig. 20c